Journal of Medicinal Chemistry

Article

Identification of SNAIL1 Peptide-Based Irreversible Lysine Specific Demethylase 1-Selective Inactivators

Yukihiro Itoh, Keisuke Aihara, Paolo Mellini, Toshifumi Tojo, Yosuke Ota, Hiroki Tsumoto, Viswas Raja Solomon, Peng Zhan, Miki Suzuki, Daisuke Ogasawara, Akira Shigenaga, Tsubasa Inokuma, Hidehiko Nakagawa, Naoki Miyata, Tamio Mizukami, Akira Otaka, and Takayoshi Suzuki

J. Med. Chem., **Just Accepted Manuscript** • DOI: 10.1021/acs.jmedchem.5b01323 • Publication Date (Web): 23 Dec 2015

Just Accepted

ACS Publications

Journal of Medicinal Chemistry is published by the American Chemical Society. 1155 Sixteenth Street N.W., Washington, DC 20036

Identification of SNAIL1 Peptide-Based Irreversible Lysine Specific Demethylase 1-Selective Inactivators

Yukihiro Itoh,[†] Keisuke Aihara,[‡] Paolo Mellini,[†] Toshifumi Tojo,[†] Yosuke Ota,[†] Hiroki Tsumoto,[#] Viswas Raja Solomon,[§] Peng Zhan,[†] Miki Suzuki,[†] Daisuke Ogasawara,[†] Akira Shigenaga,[‡] Tsubasa Inokuma,[‡] Hidehiko Nakagawa,[§] Naoki Miyata,[§] Tamio Mizukami,[¶] Akira Otaka,[‡,] and Takayoshi Suzuki[†,⊥,]**

[†]Graduate School of Medical Science, Kyoto Prefectural University of Medicine, 1-5 Shimogamohangi-Cho, Sakyo-Ku, Kyoto, 606-0823, Japan

[‡]Institute of Biomedical Sciences and Graduate School of Pharmaceutical Sciences, Tokushima University, Shomachi, Tokushima 770-8505, Japan

[§]Graduate School of Pharmaceutical Sciences, Nagoya City University, 3-1 Tanabe-dori, Mizuho-ku, Nagoya, Aichi 467-8603, Japan

[#]Research Team for Mechanism of Aging Tokyo Metropolitan Institute of Gerontology, 35-2 Sakae-Cho, Itabashi-ku, Tokyo 173-0015, Japan

[¶]Graduate School of Bio-Science, Nagahama Institute of Bio-Science and Technology, 1266 Tamura-cho, Nagahama, Shiga, 526-0829, Japan

[⊥]CREST, Japan Science and Technology Agency (JST), 4-1-8 Honcho Kawaguchi, Saitama 332-0012, Japan

ABSTRACT

Inhibition of lysine-specific demethylase 1 (LSD1), a flavin-dependent histone demethylase, has recently emerged as a new strategy for treating cancer and other diseases. LSD1 interacts physically with SNAIL1, a member of the SNAIL/SCRATCH family of transcription factors. This study describes the discovery of SNAIL1 peptide-based inactivators of LSD1. We designed and prepared SNAIL1 peptides bearing a propargyl amine, hydrazine, or phenylcyclopropane moiety. Among them, peptide **3** bearing hydrazine displayed the most potent LSD1-inhibitory activity in enzyme assays. Kinetic study and mass spectrometric analysis indicated that peptide **3** is a mechanism-based LSD1 inhibitor. Furthermore, peptides **37** and **38**, which consist of cell-membrane-permeable oligoarginine conjugated with peptide **3**, induced a dose-dependent increase of dimethylated Lys4 of histone H3 in HeLa cells, suggesting that they are likely to exhibit LSD1-inhibitory activity intracellularly. In addition, peptide **37** decreased the viability of HeLa cells. We believe this new approach for targeting LSD1 provides a basis for development of potent selective inhibitors and biological probes for LSD1.

INTRODUCTION

Chromatin modification, including DNA methylation and histone modifications such as acetylation and methylation, plays a pivotal role in transcriptional regulation.[1] These modifications epigenetically control biological functions such as cellular differentiation and developmental changes of organisms. In addition, aberrations of chromatin modification are closely associated with several diseases such as cancer and neurodegenerative disorders. Therefore, modulators that can regulate chromatin modification have attracted a great deal of attention as therapeutic agents.[2]

Among post-translation histone modifications, lysine methylation is one of the most widely studied modifications.[3] Methylation of histone lysine residues is reversible and is regulated by histone lysine methyltransferases and histone lysine demethylases (KDMs).[3,4] Lysine-specific demethylase 1 (LSD1, also known as KDM1A) is a demethylase that removes methyl groups from mono and dimethylated Lys4 of histone H3 (H3K4me1/2) through flavin adenine dinucleotide (FAD)-dependent enzymatic oxidation.[4a] LSD1 binds with several transcription factors and regulates the expression of a number of genes such as *synapsin* and *muscarinic acetylcholine receptor 4*.[5] LSD1 has also been reported to be associated with several disease states. For example, it is involved in proliferation of neuroblastoma cells and leukemia cells.[6] It is also associated with latent infection of α-herpesvirus and globin disorder.[7] Therefore, LSD1 inhibitors are of interest as chemical tools for studying the functions of LSD1 and as candidate therapeutic agents targeting LSD1.[8]

LSD1 has been reported to interact with SNAIL1, a member of the SNAIL/SCRATCH family of transcription factors, and to play a role in the expression of cancer-associated SNAIL1 target genes.[9] Further, inhibition of the interaction between LSD1 and SNAIL1 blocks cancer cell

invasion.[10] Therefore, inhibitors of the LSD1/SNAIL1 interaction appear to be novel anticancer agent candidates. Indeed, Tortorici et al. recently reported SNAIL1-derived peptides as reversible LSD1 inhibitors.[11] On the other hand, we and other groups revealed that small molecules containing a propargyl amine, hydrazine, or phenylcyclopropylamine (PCPA) moiety (Chart 1) irreversibly inhibit LSD1.[8,12] Such mechanism-based irreversible inhibitors are expected to maintain the pharmacological effect because of a long target residence time.[13] In the light of these findings, we initiated a search for SNAIL1 peptide-based irreversible LSD1 inactivators. Herein we report the design, synthesis, LSD1-inhibitory activity, and cellular activity of a series of SNAIL1-derived peptides bearing various functional groups.

CHEMISTRY

The routes used for the synthesis of peptides **1–5** (Chart 2), which were prepared for this study, are shown in Schemes 1–3. Scheme 1 shows the preparation of peptides **1** and **2** with a propargylamine moiety. Boc-Asp(OBn)-OH **6** was treated with *tert*-BuOH in the presence of EDCI and DMAP to give Boc-Asp(OBn)-O^{t}Bu **7**. The benzyl group of compound **7** was removed by hydrogenolysis to give Boc-Asp-O^{t}Bu **8**. Conversion of the carboxylic acid of **8** to mixed anhydride by using ClCOOEt and subsequent reduction with $NaBH_4$ yielded alcohol **9**. Propargylamines **11** and **12** were synthesized from the alcohol **9** via the mesylate **10**.[14] Removal of the Boc group and *tert*-butyl group of **11** and **12** using hydrochloric acid afforded amino acids **13** and **14**. Treatment of the amino acids **13** and **14** with Fmoc-OSu in the presence of $NaHCO_3$ gave the Fmoc-protected amino acids **15** and **16**, from which the propargylated peptides **1** and **2** were prepared using Fmoc-based solid-phase peptide synthesis.

Scheme 2 shows the synthesis of peptides **3** and **4**. Benzylation of aspartic acid **17** afforded Bn_2-Asp(OBn)-OBn **18**. Selective reduction of the less-hindered benzyl ester of **18** using DIBAL yielded alcohol **19**. The alcohol **19** was converted to aldehyde **20** by Swern oxidation. Reductive amino alkylation of $BocNHNH_2$ or $BocNMeNH_2$ with the aldehyde **20** in the presence of sodium cyanoborohydride gave *N*-Boc hydrazine compounds **23** and **24**. Fmoc-protected unnatural amino acids **29** and **30** were prepared from compounds **23** and **24** in three steps: Boc protection using $(Boc)_2O$, removal of the benzyl groups by hydrogenolysis, and Fmoc protection using Fmoc-OSu. The Fmoc-protected amino acids **29** and **30** were incorporated into peptides **3** and **4**, respectively, by means of Fmoc-based solid-phase peptide synthesis.

Peptide **5** was prepared from alcohol **31**[15] as outlined in Scheme 3. The alcohol **31** was reacted with mesyl chloride to obtain mesylate **32**. Treatment of the mesylate **32** with PCPA in the presence of Cs_2CO_3 gave compound **33**. Deprotection of the Boc and *tert*-butyl groups of **33** afforded amino acid **34**. The amino acid **34** was converted to Fmoc-protected PCPA-conjugated amino acid **36** by Fmoc protection of **34** and Boc protection of **35**. The PCPA-conjugated SNAIL1-based peptide **5** was prepared from **36** via standard Fmoc-based solid-phase peptide synthesis.

Oligoarginine-conjugated peptides **37**–**40** (Chart 3) were also synthesized by Fmoc-based solid-phase peptide synthesis using a lysine derivative with ivDde protection (see Experimental Section).

RESULTS AND DISCUSSION

We designed SNAIL1 peptide-based LSD1 inactivators based on the crystal structure of LSD1 complexed with a 20-amino-acid SNAIL1 *N*-terminal peptide[16] and based on the work of Cole

and co-workers on histone H3 peptide-based LSD1 inactivators containing a propargyl amine, a hydrazine, or a cyclopropylamine moiety.[12i] The X-ray crystal structure of LSD1/SNAIL1 peptide complex revealed that Phe 4 of the SNAIL1 peptide is positioned in front of the flavin in the active site of LSD1 (Figure 1). On the basis of this structure, we designed SNAIL1-based peptides **1**–**5** (Chart 2), in which the phenylalanine residue is replaced with non-natural amino acid residues bearing propargyl amine (**1** and **2**), hydrazine (**3** and **4**), or PCPA (**5**). We expected that the designed SNAIL1 peptides **1**–**5** would selectively bind LSD1 over LSD2, because it has been reported that the affinity of LSD2 for a SNAIL1 peptide at least 10 times lower than that of LSD1.[16] In addition, these SNAIL1-based peptides were expected to be recognized effectively by LSD1 (Supporting Figure S1) and to inactivate LSD1 irreversibly through amine oxidation by FAD and subsequent covalent bond formation with FAD in the active site of LSD1 (Figure 2). Specifically, peptides **1** and **2** bearing propargyl amine were expected to be oxidized to an α,β-unsaturated iminium cation species that would be nucleophilically attacked by *N*5 of the reduced FAD, leading to LSD1 inactivation (Figure 2a).[17] The expected mechanism of LSD1 inactivation by peptides **3** and **4** bearing hydrazine is shown in Figure 2b. The first oxidation of the hydrazine of peptide **3** by FAD would yield the diazene and the second oxidation of the diazene would produce the primary diazonium species, which would inactivate LSD1 through S_N2 reaction between the diazonium cation and $FADH^-$.[12i] On the other hand, peptide **4** with a monomethylhydrazine group would be converted to peptide **3** through enzymatic demethylation by LSD1. Then, it would inhibit LSD1 similarly to peptide **3**. Introduction of the methyl group into the hydrazine moiety of peptide **3** was expected to enhance the affinity for LSD1, because methylated lysine is a substrate of LSD1. The expected mechanism of LSD1 inactivation by peptide **5** involves formation of a PCPA-FAD adduct, following the oxidation by FAD and cyclopropyl ring opening (Figure 2c).[12f]

The SNAIL1-based peptides **1**–**5** were prepared (Schemes 1–3) and evaluated for LSD1-inhibitory activity using a peroxidase-coupled assay as described before.[12d,e,f] The results are summarized in Table 1 as IC_{50} values. Among the tested peptides, peptide **3** with a hydrazine moiety was found to be the most potent LSD1 inactivator (**3**: IC_{50} = 0.44 μM). The activity of peptide **4** with a monomethylhydrazine group was moderate (**4**: IC_{50} = 8.4 μM). We also examined the inhibitory activity of peptides **3** and **4** toward LSD2 which is a paralogue of LSD1, monoamine oxidase (MAO) A/B which are other FAD-dependent oxidases, and Jumonji AT-rich interactive domain 1A (JARID1A) which is one of histone H3K4me3/me2-specific demethylases.[18] As shown in Table 1, peptides **3** and **4** were inactive at concentrations up to 50 μM in LSD2-inhibitory assays. These results are consistent with the previous report that the affinity of LSD2 for SNAIL peptide is lower than that of LSD1.[16] Furthermore, the two peptides were also almost inactive against MAOs and JARID1A. These results demonstrated that peptides **3** and **4** are inhibitors with high selectivity for LSD1 over LSD2, MAO A/B and JARID1A.

Because peptide **3**, which is the most potent LSD1 inhibitor, was designed to inactivate LSD1 irreversibly as shown in Figure 2b, we next investigated the mechanism of LSD1 inhibition by peptide **3**. We initially examined whether the inhibition is time-dependent. The time course of product formation was monitored in the absence or presence of peptide **3**. As shown in Figure 3, peptide **3** was found to be a time-dependent inhibitor of LSD1.

To gain further insight into the mechanism of LSD1 inhibition by peptide **3**, mass spectrometric analysis of a mixture of LSD1 incubated with FAD and peptide **3** was performed. If peptide **3** reacts with FAD as expected, peptide **3**-FAD adduct (Figure 2b) should be generated. As depicted in Figure 4a, a significant peak at *m*/*z* 3123.4 was observed. This peak corresponds to the predicted molecular weight of peptide **3**-FAD adduct. The peak was dependent on the

presence of LSD1; that is, it was not detected in the absence of LSD1 (Figure 4b). In addition, an excess of H3K4me2 peptide, a substrate of LSD1, inhibited the generation of the **3**-FAD adduct (Supporting Figure S2). The data from the mass spectrometric analysis support the idea that peptide **3** oxidized by FAD is nucleophilically attacked by FAD^- in the active site of LSD1 to afford peptide **3**-FAD conjugate, and this reaction results in inhibition of LSD1. Kinetic analysis and mass analysis results indicate that peptide **3** is an irreversible LSD1 inactivator, as we had hoped.

Mass analysis of peptide **4** bearing a methylated hydrazine moiety was also performed. As shown in Supporting Figure S3, the peak corresponding to peptide **3**, the demethylated form of peptide **4**, was observed dependently on the presence of LSD1. In addition, the peak of peptide **3**-FAD adduct was detected dependently on LSD1, though the signal intensity was weak (Figure 4c and 4d). These results suggest that peptide **4** inhibits LSD1 through the generation of peptide **3** by demethylation of a part of peptide **4**, followed by formation of peptide **3**-FAD adduct. However, the LSD1-inhibitory activity of peptide **4** was less than that of peptide **3** (Table 1). These results indicate that the demethylation of methylated hydrazine in peptide **4** is unfavorable as compared with the oxidation of hydrazine in peptide **3**.

Although peptide compounds generally show poor cell permeability because of their high polarity, previous studies have established that oligomers of arginine covalently attached to a variety of molecules can efficiently cross the cell membrane.[19] For the application of SNAIL1-based peptide **3**, the most potent LSD1 inactivator in this study (Table 1), to cell-based assays, we therefore designed and synthesized oligoarginine-conjugated derivatives of peptide **3**. Oligoarginine-conjugated peptides **37**–**39** (Chart 3) were designed based on the X-ray crystal structure of LSD1/SNAIL1 peptide complex (Figure 5). As shown in Figure 5, the side chain of Lys 8 of the SNAIL1 peptide is located outside the active pocket of LSD1. Thus, peptides **37** and

38, in which oligoarginine is conjugated with the side chain of Lys 8 of peptide **3**, were expected to show little or no decrease of LSD1-inhibitory activity. In addition, we designed peptide **39** in which oligoarginine is conjugated with the side chain of Lys 15 of peptide **3**. It was reported that residues 10–20 of the 20-amino-acid SNAIL1 *N*-terminal peptide could not be identified in terms of electron density in the X-ray crystal structure analysis of the LSD1/SNAIL1 peptide complex.[16] This suggest that the residues 10–20 of the SNAIL1 peptide lack an ordered conformation and Lys 15 of the SNAIL1 peptide is likely to be positioned out of the active pocket of LSD1. Therefore, peptide **39** was also expected to show well-maintained LSD1-inhibitory activity, as compared with peptide **3**.

Oligoarginine-conjugated peptides **37**–**39** were prepared and initially evaluated for in vitro LSD1-inhibitory activity (Table 2). Interestingly, oligoarginine-conjugated peptides **37**–**39** were found to be more potent LSD1 inhibitors than peptide **3**. The increase in LSD1-inhibitory activity of **37** and **38** may be due to the interaction between the cationic oligoarginine and anionic amino acid residues of LSD1, such as Asp 556, Asp 557, and Glu 559 (Figure 6). Furthermore, peptides **37**–**39** displayed only weak inhibitory activity toward LSD2, MAO A/B, and JARID1A (Table 2), confirming their high selectivity for LSD1 over LSD2, MAO A/B, and JARID1A (LSD2 IC_{50}/LSD1 IC_{50} = 23–80; MAO A IC_{50}/LSD1 IC_{50} > 94; MAO B IC_{50}/LSD1 IC_{50} = 94–104; JARID1A IC_{50}/LSD1 IC_{50} = 16–44).

We also carried out mass spectrometric analysis of a mixture of LSD1 incubated with peptides **37**–**39**. The peak of peptide **37**-, **38**- or **39**-FAD adduct was detected dependently on LSD1 like the case of peptide **3** (Supporting Figure S4).

Next, we examined the activity of peptides **37**–**39** and **40** in cell-based assays. Peptide **40** (Chart 3), in which the hydrazine of peptide **37** is replaced with an amine, was prepared as a reference compound to confirm that the covalent modification is essential for the in-cell activity

of the peptides. We performed a cellular assay using western blot analysis. Because LSD1 is known to catalyze demethylation of H3K4me2, H3K4me1 and H3K9me2,[4a] the effect of oligoarginine peptides on the methylation levels of H3K4 and H3K9 in HeLa cells was examined. As shown in Figure 7a, treatment with 20 μM peptides **37** and **38** induced a large increase in dimethylated H3K4 as compared with that induced by peptides **3**, **39**, and **40**. Loss in H3K4 dimethylating activity of amine **40** suggests that the covalent bond formation of the peptide with FAD is responsible for the activity in cells. Furthermore, the increase of H3K4me2 in the presence of peptides **37** and **38** was dose-dependent without affecting the levels of H3K4me3, H3K4me1, and H3K9me2 (Figure 7b). The similar results have been obtained with the reported hydrazine-based LSD1 inhibitor.[12l] The results in both enzyme assays and cellular assays suggest that peptides **37** and **38** bearing oligoarginine moieties permeate through the cell membrane and selectively inhibit LSD1 over JARID1 in the nucleus.

Finally, we tested the effects of peptides **37**–**40** on the viability of cancer cells (Figure 8). In this study, we used HeLa cells because it has been reported that LSD1 is overexpressed in HeLa cells, and LSD1 inhibition suppresses HeLa cell growth.[12d–f] Peptide **37** reduced the cell viability at concentrations of 25–100 μM. Although peptides **38** and **39** were moderately effective, their activity was weaker than that of peptide **37**. On the other hand, peptide **40** did not inhibit the cell viability strongly. Thus, peptide **37** showed the strongest antiproliferative activity against HeLa cells among the three peptides.

CONCLUSIONS

We have designed SNAIL1-based peptides bearing a propargyl amine (**1** and **2**), hydrazine (**3** and **4**), or phenylcyclopropane (**5**) moiety based on the X-ray crystal structure of LSD1

complexed with a 20-amino-acid SNAIL1 *N*-terminal peptide. Among these five peptides, hydrazine-containing SNAIL1-based peptide **3** showed the most potent LSD1-inhibitory activity with an IC_{50} of 0.44 μM. In addition, kinetic study and mass spectrometric analysis demonstrated that peptide **3** inhibits LSD1 through covalent bond formation with FAD after oxidation of the hydrazine moiety in the active site of LSD1. Furthermore, cell-penetrating peptides **37** and **38**, which were designed based on peptide **3**, increased H3K4-methylation, suggesting that they are likely to inhibit intracellular LSD1 activity. In addition, peptide **37** decreased the viability of HeLa cells. To our knowledge, this is the first report of cell-active peptide-based LSD1 inactivators. These SNAIL1-based peptide derivatives represent an entry into a new class of LSD1-selective inhibitors, and should be useful tools for probing the biology of LSD1.

EXPERIMENTAL SECTION

Chemistry. Melting points were determined using a Yanagimoto micro melting point apparatus or a Büchi 545 melting point apparatus. Proton nuclear magnetic resonance spectra (^{1}H NMR) and carbon nuclear magnetic resonance spectra (^{13}C NMR) were recorded on a JEOL JNM-LA500, JEOL JNM-A500, BURKER AVANCE 300, or BRUKER AVANCE600 spectrometer in the indicated solvent. Chemical shifts (δ) are reported in parts per million relative to the internal standard tetramethylsilane. Electron ionization (EI) mass spectra and fast atom bombardment (FAB) mass spectra were recorded on a JEOL JMS-SX102A mass spectrometer. Electrospray ionization (ESI) mass spectra were recorded on a BRUKER HCTplus mass spectrometer (ESI-IT) or a Waters MICROMASS® LCT PREMIER™ (ESI-TOF). The specific rotation was measured on a HORIBA SEPA-300 polarimeter. HPLC analysis for unnatural amino acids was performed on a Cosmosil 5C_{18}-AR-II analytical column (Nacalai Tesque, 4.6 ×

250 mm, flow rate 1.0 mL/min) and eluted products were detected by UV absorbance measurement at 254 nm. A solvent system consisting of 0.1% (v/v) TFA aqueous solution (solvent A) and 0.1% (v/v) TFA in MeCN (solvent B) was used for HPLC elution. For HPLC separation of synthetic peptides, a Cosmosil 5C_{18}-AR-II analytical column (Nacalai Tesque, 4.6 × 250 mm, flow rate 1.0 mL/min) or a Cosmosil 5C_{18}-AR-II preparative column (Nacalai Tesque, 20 × 250 mm, flow rate 10 mL/min) was employed and eluted products were detected by UV absorbance measurement at 220 nm. A solvent system consisting of 0.1% (v/v) TFA aqueous solution (solvent A) and 0.1% (v/v) TFA in MeCN (solvent B) was used for HPLC elution. Chiral HPLC was performed on a CHIRALPAK IA column (4.6 × 250 mm, flow rate 1 mL/min) and eluted products were detected by UV absorbance measurement at 254 nm. A solvent system consisting of hexane/*i*PrOH = 90/10 (v/v) was used for chiral HPLC elution. The purity of the unnatural amino acid compounds for peptide synthesis and the tested peptides was determined by HPLC and the purity level was ≥95%. Reagents and solvents were purchased from Aldrich, Tokyo Kasei Kogyo, Wako Pure Chemical Industries, and Kanto Kagaku and used without purification. Flash column chromatography was performed using silica gel supplied by Merck or Toyota Silica Gel.

Fmoc-based solid-phase peptide synthesis. An Fmoc-protected amino acid (5.0 eq.) was coupled to NovaSyn® TGR resin (0.25 mmol amine/g), which affords peptide amide, with the aid of *N*,*N*′-diisopropylcarbodiimide (5.0 eq.) and 1-hydroxy-1*H*-benzotriazole monohydrate (5.0 eq.) in DMF at room temperature for 2 h. Then the Fmoc group was removed with 20% (v/v) piperidine in DMF at room temperature for 10 min. After peptide chain elongation, Boc-Pro-OH was introduced as an N-terminal residue. The resulting resin was treated with TFA/*m*-cresol/thioanisole/1,2-ethanedithiol/H_2O (80/5/5/5/5 (v/v), 50 μL/1 mg resin) at room temperature for 1.5 h. After removal of the resin by filtration, cooled Et_2O was added to the

filtrate, and the precipitate was collected by centrifugation. The precipitate was washed with Et_2O, and the obtained crude peptide was purified by preparative HPLC and then lyophilized. All purified peptides were obtained as white lyophilized powders. For introduction of an oligoarginine unit, an *N*-ε-[1-(4,4-dimethyl-2,6-dioxocyclohex-1-ylidene)-3-methylbutyl] (ivDde) group was used as a protecting group for a side chain of lysine. Fmoc-Lys(ivDde)-OH was incorporated at the site of Lys8 or Lys15. After sequence elongation, the ivDde group was removed by treatment with 4% (v/v) hydrazine monohydrate in DMF at room temperature for 5 h. Then, oligoarginine (R8) or an oligoarginine (R8)-miniPEG^{TM} was introduced on the generated ε–amine using standard Fmoc-based solid-phase peptide synthesis as described above. Results of characterization of peptides are presented in the supporting information.

SNAIL1-20-peptide-based propargylbenzylamine (1). Step 1: Preparation of (*S*)-5-benzyl 1-*tert*-butyl 2-*tert*-butoxycarbonylaminopentanedioate (7). A solution of (*S*)-5-benzyloxy-2-*tert*-butoxycarbonylamino-5-oxopentanoic acid (**6**) (6.00 g, 17.8 mmol), *tert*-butanol (1.70 mL, 18.0 mmol), EDCI (3.45 g, 18.0 mmol), and DMAP (2.20 g, 18.0 mmol) in CH_2Cl_2 (60 mL) was stirred at room temperature for 12 hours. The reaction mixture was washed with saturated aqueous $NaHCO_3$ and brine, and dried over Na_2SO_4. Filtration, concentration in vacuo, and purification of the residue by flash column chromatography (AcOEt/*n*–hexane = 1/9) gave 6.50 g (93%) of **7** as a colorless oil: ^{1}H NMR (CD_3OD, 500 MHz, δ; ppm) 7.35–7.30 (5H, m), 5.12 (2H, s), 4.03–4.00 (1H, m), 2.47–2.44 (2H, m), 2.14–2.07 (1H, m), 1.89–1.84 (1H, m), 1.45 (9H, s), 1.43 (9H, s); MS (EI) *m/z*: 393 (M^+); $[\alpha]^{24}_D$ -6.74 (c 0.089, MeOH).

Step 2: Preparation of (*S*)-5-*tert*-butoxy-4-*tert*-butoxycarbonylamino-5-oxopentanoic acid (8). To a solution of **7** (6.00 g, 15.3 mmol) in MeOH (3 mL) was added 850 mg of 5% Pd/C. The mixture was stirred under H_2 at room temperature for 8 hours, and then filtered through Celite®.

The filtrate was concentrated in vacuo to give 4.50 g (97%) of **8** as a colorless oil: ^{1}H NMR (CD_3OD, 500 MHz, δ; ppm) 4.02–3.99 (1H, m), 2.38 (2H, t, J = 7.5 Hz), 2.08–2.04 (1H, m), 1.88–1.81 (1H, m), 1.47 (9H, s), 1.44 (9H, s); MS (EI) *m/z*: 303 (M^+); $[\alpha]^{23}_D$ -12.22 (c 0.090, MeOH).

Step 3: Preparation of (*S*)-*tert*-butyl 2-*tert*-butoxycarbonylamino-5-hydroxypentanoate (9). To a solution of **8** (1.53 g, 5.06 mmol) and triethylamine (3.5 mL, 25.1 mmol) in THF (21 mL) was added ethyl chloroformate (2.5 mL, 26.1 mmol) at –10 °C. The mixture was stirred at –10 °C for 1 hour and insoluble materials were filtered off. To a solution of $NaBH_4$ (956 mg, 25.3 mmol) in THF (20 mL) and water (5 mL) was added the filtrate at 0 °C, and the reaction mixture was stirred at room temperature for 5 hours. After acidification with 1 N aqueous HCl (to pH 3), the mixture was extracted with AcOEt. The organic layer was separated, washed with 10% aqueous solution of NaOH, water, and brine, and dried over Na_2SO_4. Filtration, concentration in vacuo, and purification of the residue by flash column chromatography (AcOEt/*n*–hexane = 1/3) gave 1.08 g (74%) of **9** as a colorless oil: ^{1}H NMR (CD_3OD, 500 MHz, δ; ppm) 3.96–3.94 (1H, m), 3.56–3.53 (2H, m), 1.86–1.80 (1H, m), 1.68–1.64 (1H, m), 1.60–1.55 (2H, m), 1.46 (9H, s), 1.44 (9H, s); MS (EI) *m/z*: 289 (M^+); $[\alpha]^{23}_D$ -5.62 (c 0.169, MeOH).

Step 4: Preparation of (*S*)-*tert*-butyl 2-*tert*-butoxycarbonylamino-5-methylsulfonyloxypentanoate (10). To a solution of **9** (500 mg, 1.73 mmol), triethylamine (3.5 mL, 25.1 mmol), and DMAP (21.0 mg, 0.173 mmol) in CH_2Cl_2 (3 mL) was added dropwise methanesulfonyl chloride (270 μL, 3.46 mmol) at –20 °C. The reaction mixture was stirred at –20 °C for 1 hour, then poured into water and extracted with AcOEt. The organic layer was separated, washed with brine, and dried over Na_2SO_4. Filtration, concentration in vacuo, and purification of the residue by flash column chromatography (AcOEt/*n*–hexane = 1/1) gave 370

mg (58%) of **10** as a colorless oil: ^{1}H NMR (CD_3OD, 500 MHz, δ; ppm) 4.25 (2H, t, J = 6.5 Hz), 4.00–3.98 (1H, m), 3.06 (1H, s), 1.92–1.85 (1H, m), 1.83–1.77 (2H, m), 1.74–1.66 (1H, m), 1.46 (9H, s), 1.44 (9H, s); MS (EI) *m/z*: 367 (M^+).

Step 5: Preparation of (*S*)-*tert*-butyl 5-benzyl(prop-2-yn-1-yl)amino-2-*tert*-butoxycarbonylaminopentanoate (11). To a solution of **10** (368 mg, 1.00 mmol) in DMF (1 mL) was added benzylpropargylamine (217 mg, 1.50 mmol) and Cs_2CO_3 (500 mg, 1.50 mmol) and the reaction mixture was stirred at 65 °C for 2 hours. The reaction mixture was poured into water and extracted with $CHCl_3$. The organic layer was separated and washed with saturated aqueous $NaHCO_3$ and brine, and dried over Na_2SO_4. Filtration, concentration in vacuo, and purification of the residue by flash column chromatography (AcOEt/*n*–hexane = 1/1) gave 70 mg (19%) of **11** as a colorless oil: ^{1}H NMR (CD_3OD, 500 MHz, δ; ppm) 7.34 (2H, d, J = 7.5 Hz), 7.28–7.25 (3H, m), 4.58 (2H, s), 4.16 (2H, s), 4.04–4.03 (2H, s), 4.00–3.99 (2H, m), 2.65 (1H, d, J = 2.5 Hz), 1.70–1.68 (4H, m), 1.46 (9H, s), 1.44 (9H, s); MS (EI) *m/z*: 416 (M^+).

Step 6: Preparation of (*S*)-2-amino-5-benzyl(prop-2-yn-1-yl)aminopentanoic acid hydrochloric acid salt (13·HCl). To a solution of **11** (500 mg, 1.20 mmol) in CH_2Cl_2 (2 mL) was added dropwise 4 N HCl in dioxane (5 mL, 20.0 mmol) at 0 °C. The reaction mixture was stirred at 0 °C for 1 hour, and then concentrated in vacuo to give 330 mg (80%) of **13·HCl** as a colorless amorphous solid: ^{1}H NMR (CD_3OD, 500 MHz, δ; ppm) 7.58 (2H, broad s), 7.33 (2H, d, J = 7.5 Hz), 7.29–7.28 (3H, m), 4.58 (2H, s), 4.21 (2H, s), 4.04–3.98 (4H, m), 2.66 (1H, d, J = 2.5 Hz), 2.11–1.98 (4H, m); MS (EI) *m/z*: 260 (M^+).

Step 7: Preparation of (*S*)-2-[(9*H*-fluoren-9-yl)methoxy]carbonylamino-5-benzyl(prop-2-yn-1-yl)aminopentanoic acid (15). To a solution of **13·HCl** (330 mg, 1.27 mmol) and $NaHCO_3$ (640 mg, 7.61 mmol) in water (2 mL) and dioxane (1 mL) was added *N*-(9-

fluorenylmethoxycarbonyloxy)succinimide (427 mg, 1.27 mmol) in dioxane (1 mL) at 0 °C. The reaction mixture was stirred at room temperature for 15 hour. After acidification with 2 N aqueous HCl (to pH 6), the mixture was extracted with AcOEt. The organic layer was separated, washed with brine and dried over Na_2SO_4. Filtration, concentration in vacuo, and purification of the residue by flash column chromatography ($CHCl_3$/MeOH = 1/9) gave 120 mg (20%) of **15** as a colorless solid: ^{1}H NMR (CD_3OD, 500 MHz, δ; ppm) 7.79 (2H, d, *J* = 7.5 Hz), 7.68 (2H, d, *J* = 7.5 Hz), 7.39 (2H, d, *J* = 7.5 Hz), 7.31–7.28 (5H, m), 7.27–7.25 (2H, m), 4.57 (2H, s), 4.37–4.35 (2H, m), 4.22–4.17 (4H, m), 4.05–3.98 (2H, m), 2.65 (1H, d, *J* = 2.5 Hz), 2.12–1.98 (2H, m), 1.81–1.77 (2H, m); MS (EI) *m/z*: 482 (M^+); HPLC, retention time = 43.4 min, purity 95.6% (analytical HPLC conditions: a linear gradient, 0 min (5% B)-45 min (50% B)-55 min (50% B)-60 min (90% B)); $[\alpha]^{20}_D$ +6.94 (c 0.072, MeOH).

Step 8: Preparation of SNAIL1-20-peptide-based propargylbenzylamine (1). By employing **15**, peptide **1** was obtained in 17% isolated yield based on the starting resin: HPLC, retention time = 19.4 min, purity 96.0% (analytical HPLC conditions: linear gradient of solvent B in solvent A, 5 to 30% over 30 min); preparative HPLC conditions: linear gradient of solvent B in solvent A 13% to 23% over 30 min); LRMS (ESI-TOF) *m/z* calcd for $C_{111}H_{177}N_{35}O_{30}$ ([M + 3H]$^{3+}$): 827.8, found: 827.6.

SNAIL1-20-peptide-based propargylmethylamine (2). **Preparation of (*S*)-2-({[(9*H*-fluoren-9-yl)methoxy]carbonyl}amino)-5-[methyl(prop-2-yn-1-yl)amino]pentanoic acid (16).** Compound **16** was prepared from **10** using the procedure described for **1** (steps 5–7, yield 4.0% from **10**): ^{1}H NMR (500 MHz, CD_3OD, δ; ppm): 7.88 (2H, d, *J* = 7.5 Hz), 7.71–7.64 (2H, m), 7.37 (2H, t, *J* = 7.5 Hz), 7.29 (2H, t, *J* = 7.5 Hz), 4.33 (2H, m), 4.19 (1H, t, *J* = 6.5 Hz), 4.07 (1H, q, *J* = 4.5 Hz), 3.78 (2H, d, *J* = 2.5 Hz), 3.05 (1H, t, *J* = 2.5 Hz), 2.90–2.87 (2H, m), 2.65 (3H, s),

1.86–1.83 (1H, m), 1.72–1.61 (2H, m), 1.41–1.38 (2H, m); ^{13}C NMR (125 MHz, $CDCl_3$, δ; ppm): 177.88, 158.40, 145.26, 128.22, 128.20, 126.30, 120.96, 78.64, 75.44, 68.01, 57.01, 56.51, 56.37, 45.96, 41.06, 33.11, 26.10, 24.06; MS (FAB) *m/z*: 423 (MH^+); HPLC, retention time = 25.2 min, purity 99.2% (analytical HPLC conditions: a linear gradient, 0 min (5% B)-25 min (50% B)-35 min (50% B)-40 min (90% B)-50 min (90% B)); $[\alpha]^{22}_D$ +2.19 (c 0.228, MeOH).

Preparation of SNAIL1-20-peptide-based propargylmethylamine (2). By employing **16**, peptide **2** was obtained in 16% isolated yield based on the starting resin: HPLC, retention time = 15.9 min, purity 96.8% (analytical HPLC conditions: linear gradient of solvent B in solvent A, 5 to 30% over 30 min); preparative HPLC conditions: linear gradient of solvent B in solvent A 6% to 16% over 30 min); LRMS (ESI-TOF) *m/z* calcd for $C_{105}H_{173}N_{35}O_{30}$ ($[M + 3H]^{3+}$): 802.4, found: 802.2.

SNAIL1-20-peptide-based hydrazine (3). Step 1: Preparation of (*S*)-dibenzyl 2-(dibenzylamino)pentanedioate (18). To a solution of L-glutamic acid (**17**) (4.26 g, 29.0 mmol), K_2CO_3 (16.2 g, 118 mmol), and NaOH (2.33 g, 58.0 mmol) in water (100 mL) was slowly added benzyl bromide (20.2 g, 118 mmol). The reaction mixture was stirred at reflux temperature for 3 hours, and then extracted with AcOEt. The organic layer was separated and dried over Na_2SO_4. Filtration, concentration in vacuo, and purification of the residue by flash column chromatography (AcOEt/*n*–hexane = 1/9) gave 4.31 g (29%) of **18** as a colorless oil: ^{1}H NMR (300 MHz, $CDCl_3$, δ; ppm): 7.45–7.18 (20H, m), 5.23 (1H, d, *J* = 12.3 Hz), 5.22 (1H, d, *J* = 12.3 Hz), 5.00 (1H, d, *J* = 12.6 Hz), 5.00 (1H, d, *J* = 12.6 Hz), 4.95 (1H, d, *J* = 12.6 Hz), 3.88 (2H, d, *J* = 13.8 Hz), 3.50 (2H, d, *J* = 13.8 Hz), 3.41 (1H, t, *J* = 7.7 Hz), 2.50 (1H, m), 2.34 (1H, m), 2.05 (2H, m); ^{13}C NMR (75 MHz, $CDCl_3$, δ; ppm): 173.53, 172.91, 139.95, 136.70, 129.65, 129.37, 129.28, 129.24, 129.11, 129.05, 128.92, 127.82, 66.95, 66.90, 60.60, 55.23, 31.42, 25.05; MS

(ESI-IT) *m/z*: 508 [(M+H)$^+$]; $[\alpha]^{23}_D$ -83.52 (c 0.182, MeOH).

Step 2: Preparation of (*S*)-benzyl 2-(dibenzylamino)-5-hydroxypentanoate (19). To a solution of **18** (1.92 g, 3.78 mmol) in THF (12.5 mL) was slowly added DIBAL (8.32 mL of a 1 M solution in toluene, 8.32 mmol) at –15 °C. The reaction mixture was stirred at 0 °C for 30 minutes, and then water (7 mL) was added. Stirring was continued at 0 °C for 30 minutes. Filtration, concentration in vacuo, and purification of the residue by flash column chromatography (AcOEt/*n*–hexane = 1/4 to 1/2) gave 1.40 g (92%) of **19** as a colorless oil: ^{1}H NMR (300 MHz, $CDCl_3$, δ; ppm): 7.45–7.34 (5H, m), 7.33–7.18 (10H, m), 5.26 (1H, d, *J* = 12.3 Hz), 5.14 (1H, d, *J* = 12.3 Hz), 3.93 (2H, d, *J* = 14.1 Hz), 3.50 (1H, d, *J* = 13.5 Hz), 3.54–3.43 (4H, m), 3.38 (1H, t, *J* = 7.5 Hz), 1.87–1.61 (3H, m), 1.58–1.39 (1H, m), 1.30 (1H, br); ^{13}C NMR (75 MHz, $CDCl_3$, δ; ppm): 173.48, 140.18, 136.83, 129.68, 129.37, 129.28, 129.02, 127.81, 66.81, 63.18, 61.36, 55.29, 30.10, 26.58; MS (ESI-IT) *m/z*: 404 [(M+H)$^+$]; $[\alpha]^{24}_D$ -111.54 (c 0.117, MeOH).

Step 3: Preparation of (*S*)-benzyl 2-(dibenzylamino)-5-oxopentanoate (20). To a solution of oxalyl chloride (690 μL, 7.92 mmol) in CH_2Cl_2 (3mL) was slowly added a solution of DMSO (675 μL, 9.50 mmol) in CH_2Cl_2 (2 mL) at –78 °C. The mixture was stirred for 25 minutes at –78 °C, then a solution of **19** (1.28 g, 3.17 mmol) in CH_2Cl_2 (2 mL) at –78 °C was slowly added, and stirring was continued for 2 hours at –78 °C. To the mixture was added Et_3N (1.3 mL, 9.38 mmol), and stirring was continued for 1 hour at –78 °C. The mixture was further stirred for 15 minutes 0 °C, then poured into water, and extracted with CH_2Cl_2. The organic layer was separated, washed with brine, and dried over Na_2SO_4. Filtration, concentration in vacuo and purification of the residue by flash column chromatography (AcOEt/*n*–hexane = 1/9 to 1/2) gave 1.08 g (85%) of **20** as a colorless oil: ^{1}H NMR (300 MHz, $CDCl_3$, δ; ppm): 9.59 (1H, t, *J* = 1.2

Hz), 7.46–7.35 (5H, m), 7.34–7.20 (10H, m), 5.27 (1H, d, J = 12.3 Hz), 5.17 (1H, d, J = 12.3 Hz), 3.87 (2H, d, J = 13.8 Hz), 3.50 (2H, d, J = 13.8 Hz), 3.35 (1H, t, J = 7.8 Hz), 2.60–2.32 (2H, m), 2.08–1.98 (2H, m); ^{13}C NMR (75 MHz, $CDCl_3$, δ; ppm): 201.38, 172.12, 139.12. 135.95, 128.93, 128.67, 128.58, 128.45, 128.36, 127.19, 66.27, 59.87, 54.54, 40.47, 21.66; MS (ESI-IT) *m/z*: 402 [$(M+H)^+$]; $[\alpha]^{22}_D$ -72.22 (c 0.126, MeOH).

Step 4: Preparation of (*S*)-*tert*-butyl 2-[5-(benzyloxy)-4-(dibenzylamino)-5-oxopentylidene]hydrazinecarboxylate (21). To a solution of **20** (382 mg, 0.951 mmol) in THF (10 mL) was added *tert*-butyl carbazate (257 mg, 1.94 mmol). The mixture was stirred for 5 hours at room temperature, then diluted with AcOEt, washed with brine, and dried over Na_2SO_4. Filtration, concentration in vacuo, and purification of the residue by flash column chromatography (AcOEt/*n*–hexane = 1/5 to 1/2) gave 459 mg (94%) of **21** as a colorless oil: ^{1}H NMR (300 MHz, $CDCl_3$, δ; ppm), small rotamers observed but not reported: 7.43–7.32 (5H, m), 7.30–7.18 (10H, m), 6.78 (1H, m), 5.27 (1H, d, J = 12.3 Hz), 5.17 (1H, d, J = 12.3 Hz), 3.88 (2H, d, J = 13.8 Hz), 3.50 (2H, d, J = 13.8 Hz), 3.38 (1H, m), 2.50–2.36 (1H, m), 2.28–2.16 (1H, m), 2.05–1.84 (2H, m), 1.49 (9H, s); ^{13}C NMR (75 MHz, $CDCl_3$, δ; ppm), small rotamers observed but not reported: 171.37, 138.40, 135.09, 128.08, 128.01, 127.80, 127.73, 127.64, 127.49, 127.42, 126.18, 80.12, 65.26, 58.99, 53.54, 27.84, 27.39, 25.44; MS (ESI-IT) *m/z*: 516 [$(M+H)^+$].

Step 5: Preparation of (*S*)-*tert*-butyl 2-[5-(benzyloxy)-4-(dibenzylamino)-5-oxopentyl]hydrazinecarboxylate (23). To a solution of **21** (230 mg, 0.446 mmol) in EtOH (5 mL) were added acetic acid (500 μL, 8.74 mmol) and sodium cyanoborohydride (138 mg, 1.98 mmol). The reaction mixture was stirred for 12 hours at room temperature, then diluted with AcOEt, washed with aqueous saturated sodium bicarbonate and brine, and dried over Na_2SO_4. Filtration, concentration in vacuo, and purification of the residue by flash column

chromatography (AcOEt/*n*–hexane = 1/4 to 1/1) gave 160 mg (69%) of **23** as a colorless oil: ^{1}H NMR (300 MHz, $CDCl_3$, δ; ppm): 7.45–7.35 (5H, m), 7.32–7.18 (10H, m), 5.85 (1H, br), 5.26 (1H, d, *J* = 12.3 Hz), 5.14 (1H, d, *J* = 12.3 Hz), 3.88 (2H, d, *J* = 13.8 Hz), 3.50 (2H, d, *J* = 13.8 Hz), 3.35 (1H, t, *J* = 7.5 Hz), 2.68 (2H, t, *J* = 7.0 Hz), 1.86–1.73 (2H, m), 1.60 (13H, m); ^{13}C NMR (75 MHz, $CDCl_3$, δ; ppm): 168.82, 135.65, 132.21, 124.69, 124.58, 124.41, 124.34, 123.07, 76.47, 62.06, 56.78, 50.58, 47.61, 24.46, 23.04, 20.48; MS (ESI-IT) *m/z*: 518 [$(M+H)^+$].

Step 6: Preparation of (*S*)-*tert*-butyl 2-[5-(benzyloxy)-4-(dibenzylamino)-5-oxopentyl]hydrazinecarboxylate (25). To a solution of **23** (160 mg, 0.309 mmol) in CH_2Cl_2 (5 mL) were added di-*tert*-butyl dicarbonate (82.1 mg, 0.376 mmol) and 4-dimethylaminopyridine (10.2 mg). The mixture was stirred at room temperature for 7 hours, then diluted with CH_2Cl_2, washed with water and brine, and dried over Na_2SO_4. Filtration, concentration in vacuo, and purification of the residue by flash column chromatography (AcOEt/*n*–hexane = 1/4) gave 148 mg (78%) of **25** as a colorless oil: ^{1}H NMR (300 MHz, $CDCl_3$, δ; ppm) 7.52–7.35 (5H, m), 7.32–7.18 (10H, m), 5.26 (1H, d, *J* = 12.3 Hz), 5.12 (1H, d, *J* = 12.3 Hz), 4.38 (1H, br), 3.89 (2H, d, *J* = 13.8 Hz), 3.49 (2H, d, *J* = 13.8 Hz), 3.35 (1H, t, *J* = 7.3 Hz), 2.70 (2H, t, *J* = 7.3 Hz), 1.86–1.35 (22H, m); ^{13}C NMR (75 MHz, $CDCl_3$, δ; ppm): 172.64, 152.37, 139.50, 136.12, 128.84, 128.60, 128.49, 128.31, 128.26, 126.98, 83.06, 65.97, 60.79, 54.46, 50.88, 28.20, 28.09, 27.11, 24.51; MS (ESI) *m/z*: 618 [$(M+H)^+$].

Step 7: Preparation of (*S*)-2-amino-5-[1,2-bis(*tert*-butoxycarbonyl)hydrazinyl]pentanoic acid (27). To a solution of **25** (185 mg, 0.299 mmol) in MeOH (20 mL) was added a solution of formic acid (260 μL) in MeOH (8.7 mL) and palladium black (100 mg, high surface area, 99.8%) at –40 °C. The reaction mixture was stirred at room temperature for 2 hours. The palladium was filtered off and the filtrate was concentrated in vacuo to give 125 mg of crude **27** which was used

for the next step without further purification: MS (ESI-IT) *m/z*: 348 [$(M+H)^+$]; $[\alpha]^{25}_D$ -50.00 (c 0.030, MeOH).

Step 8: Preparation of (*S*)-2-[(9*H*-fluoren-9-ylmethoxycarbonyl)amino]-5-[1,2-bis(*tert*-butoxycarbonyl)hydrazinyl]pentanoic acid (29). To a solution of crude **27** (125 mg) and $NaHCO_3$ (151 mg, 1.80 mmol) in water (1.5 mL) and dioxane (3 mL) was added *N*-(9-fluorenylmethoxycarbonyloxy)succinimide (242 mg, 0.720 mmol) in dioxane (1 mL) at 0 °C. The reaction was stirred at room temperature for 3 hours. After acidification with 10% citric acid, the mixture was extracted with AcOEt. The organic layer was separated, washed with brine and dried over Na_2SO_4. Filtration, concentration in vacuo, and purification of the residue by flash column chromatography ($MeOH/CH_2Cl_2$ = 1/99 to 1/6) followed by preparative TLC ($MeOH/CH_2Cl_2$ = 1/12) gave 151 mg (89%, 2 steps) of **29** as a colorless solid: ^1H NMR ($CDCl_3$, 300 MHz, δ; ppm), small rotamers observed but not reported: 7.74 (2H, d, *J* = 7.2 Hz), 7.59 (2H, m), 7.38 (2H, t, *J* = 7.2 Hz), 7.29 (2H, t, *J* = 7.2 Hz), 5.89 (1H, brd, *J* = 7.2 Hz), 4.60–4.32 (3H, m), 4.20 (1H, m), 2.87 (2H, m), 2.02–1.85 (2H, m), 1.81–1.69 (2H, m), 1.50 (18H, s); ^{13}C NMR (75 MHz, $CDCl_3$, δ; ppm), small rotamers observed but not reported: 156.21, 152.32, 143.97, 143.84, 141.84, 127.66, 127.08, 125.20, 119.92, 83.94, 67.09, 53.86, 50.36, 47.16, 29.96, 28.05, 23.06; MS (ESI-IT) m/z: 570 [$(M+H)^+$]; HPLC, retention time = 20.2 min, purity 96.7% (rotamer mixture) (analytical HPLC conditions: a linear gradient, 0 min (50% B)-30 min (50% B)-35 min (90% B)-40 min (90% B)); $[\alpha]^{20}_D$ +1.90 (c 0.079, MeOH); Chiral HPLC, >99% ee, retention time = 59.0 min (major, *S* form), 28.0 min (minor, *R* form) (This compound was protected as methyl ester by using trimethylsilyldiazomethane[20] and the ester form was analyzed by chiral HPLC).

Step 9: Preparation of SNAIL1-20-peptide-based hydrazine (3). By employing **29**, peptide

3 was obtained in 16% isolated yield based on the starting resin: HPLC, retention time = 18.0 min, purity 97.7% (analytical HPLC conditions: linear gradient of solvent B in solvent A, 1 to 30% over 30 min); preparative HPLC conditions: linear gradient of solvent B in solvent A 6% to 16% over 30 min); LRMS (ESI-TOF) *m/z* calcd for $C_{101}H_{170}N_{36}O_{30}$ ($[M + 3H]^{3+}$): 790.1, found: 789.9.

SNAIL1-20-peptide-based hydrazine (4): Preparation of (*S*)-2-({[(9*H*-fluoren-9-yl)methoxy]carbonyl}amino)-5-[1,2-bis(*tert*-butoxycarbonyl)-2-methylhydrazinyl]pentanoic acid (30). Compound **30** was prepared from **20** using the procedure described for **3** (steps 5–8, yield 28% from **20**): ^{1}H NMR (DMSO, 300 MHz, δ; ppm), small rotamers observed but not reported: 12.61 (1H, br), 7.89 (2H, d, *J* = 7.6 Hz), 7.65–7.63 (3H, m), 7.41 (2H, t, *J* = 7.6 Hz), 7.32 (2H, t, *J* = 7.6 Hz), 4.26–4.21 (3H, m), 4.07–3.96 (1H, m), 2.95 (3H, m), 1.83–1.68 (1H, m), 1.66–1.49 (3H, m), 1.41–1.34 (18H, m); ^{13}C NMR (75 MHz, $CDCl_3$, δ; ppm), small rotamers observed but not reported: 175.95, 156.66, 155.91, 155.24, 143.91, 141.34, 127.76, 127.13, 125.19, 120.01, 81.61, 67.27, 53.64, 48.19, 47.19, 37.45, 29.86, 28.33, 24.34; MS (ESI-IT) m/z: 584 (MH^+); HPLC, retention time = 18.6 min, purity 98.3% (analytical HPLC conditions: a linear gradient, 0 min (50% B)-30 min (90% B)-40 min (90% B)); $[\alpha]^{20}_{D}$ +4.11 (c 0.073, MeOH).

Preparation of SNAIL1-20-peptide-based hydrazine (4): By employing **30**, peptide **4** was obtained in 29% isolated yield based on the starting resin: HPLC, retention time = 18.2 min, purity 96.0% (analytical HPLC conditions: linear gradient of solvent B in solvent A, 1 to 30% over 30 min); preparative HPLC conditions: linear gradient of solvent B in solvent A 6% to 16% over 30 min); LRMS (ESI-TOF) *m/z* calcd for $C_{102}H_{172}N_{36}O_{30}$ ($[M + 3H]^{3+}$): 794.8, found: 794.6.

SNAIL1-20-peptide-based phenylcyclopropylamine (5). Preparation of (2*S*)-2-({[(9*H*-fluoren-9-yl)methoxy]carbonyl}amino)-6-[(*tert*-butoxycarbonyl)(2-phenylcyclopropyl)

amino]hexanoic acid (36). Compound **36** was prepared from **31**[16] using the procedure described for **1** (steps 4–7) and **3** (step 6): yield 2%; ^{1}H NMR (500 MHz, CD_3OD, δ; ppm) 7.90 (2H, t, *J* = 7.5 Hz), 7.78 (2H, d, *J* = 7.5 Hz), 7.39 (2H, d, *J* = 7.0 Hz), 7.29–7.27 (2H, m), 7.22–7.19 (2H, m), 7.12 (2H, d, *J* = 8.0 Hz), 7.09–7.06 (1H, m), 4.59–4.58 (1H, m), 4.20–4.18 (1H, m), 4.04–4.01 (1H, m), 2.57–2.56 (1H, m), 2.07–2.06 (1H, m), 1.51–1.42 (6H, m), 1.40 (9H, s), 1.28–1.12 (4H, m); MS (FAB): *m/z* 585 $[(M+H)^+]$; ^{13}C NMR (500 MHz, CD_3OD, δ; ppm) HPLC, retention time = 25.8 min, purity 97.0% (analytical HPLC conditions: a linear gradient, 0 min (10% B)-15 min (75% B)-35 min (75% B); $[\alpha]^{20}_D$ +0.197 (c 0.254, MeOH).

Preparation of SNAIL1-20-peptide-based phenylcyclopropylamine (5). By employing **36**, peptide **5** was obtained in 14% isolated yield from the starting resin: HPLC, retention time = 15.8 min, purity 95.2% (analytical HPLC conditions: linear gradient of solvent B in solvent A, 5 to 45% over 30 min); preparative HPLC conditions: linear gradient of solvent B in solvent A 15% to 25% over 30 min); LRMS (ESI-TOF) m/z calcd for $C_{111}H_{179}N_{35}O_{30}$ ($[M + 3H]^{3+}$): 828.8, found: 828.5.

Oligoarginine-conjugated peptide 37. Peptide **37** was prepared according to the general procedure and was obtained in 10% isolated yield from the starting resin: retention time = 19.2 min, purity 95.0% (analytical HPLC conditions: linear gradient of solvent B in solvent A, 1 to 30% over 30 min); preparative HPLC conditions: linear gradient of solvent B in solvent A 8% to 18% over 30 min); LRMS (ESI-TOF) *m/z* calcd for $C_{149}H_{266}N_{68}O_{38}$ ($[M + 4H]^{4+}$): 905.0, found: 904.8.

Oligoarginine-conjugated peptide 38. Peptide **38** was prepared according to the general procedure and was obtained in 10% isolated yield from the starting resin: HPLC, retention time = 19.6 min, purity 95.5% (analytical HPLC conditions: linear gradient of solvent B in solvent A, 1

to 30% over 30 min); preparative HPLC conditions: linear gradient of solvent B in solvent A 8% to 18% over 30 min); LRMS (ESI-TOF) *m/z* calcd for $C_{155}H_{277}N_{69}O_{41}$ ($[M + 4H]^{4+}$): 941.3, found: 941.1.

Oligoarginine-conjugated peptide 39. Peptide **39** was prepared according to the general procedure and was obtained in 21% isolated yield from the starting resin: HPLC, retention time = 18.8 min, purity 97.5% (analytical HPLC conditions: linear gradient of solvent B in solvent A, 1 to 30% over 30 min); preparative HPLC conditions: linear gradient of solvent B in solvent A 7% to 17% over 30 min); LRMS (ESI-TOF) *m/z* calcd for $C_{149}H_{266}N_{68}O_{38}$ ($[M + 4H]^{4+}$): 905.0, found: 904.9.

Oligoarginine-conjugated peptide 40. Peptide **40** was prepared according to the general procedure and was obtained in 33% isolated yield from the starting resin: HPLC, retention time = 20.0 min, purity 97.3% (analytical HPLC conditions: linear gradient of solvent B in solvent A, 1 to 30% over 30 min); preparative HPLC conditions: linear gradient of solvent B in solvent A 8% to 30% over 30 min); LRMS (ESI-TOF) m/z calcd for $C_{150}H_{267}N_{67}O_{38}$ ($[M + 4H]^{4+}$): 904.8, found: 904.3.

Biology. ***LSD1 Inhibition Assay.*** LSD1 activity was assayed at 25°C by using the peroxidase-coupled method, as described previously.[11d,e,f] The chemically synthesized peptide consisting of the first 21 amino acid residues of histone H3, incorporating dimethylated lysine at position 4 (H3K4me2 peptide) (Sigma-Aldrich), was used as the substrate of LSD1. The reaction mixture contained 50 mM HEPES-NaOH, pH 7.5, 0.1 mM 4-aminoantipyrine, 1 mM 3,5-dichloro-2-hydroxybenzenesulfonic acid, 5.5 units/ml horseradish peroxidase, 20 μM H3K4me2 peptide, and an appropriate amount of LSD1. To assess the inhibitory effect of test compounds on the LSD1 activity, we used partially purified LSD1 (obtained at the purification step of HisTrap HP chromatography) dissolved in buffer C. Reaction in the absence of inhibitors was also done as a

control. Reaction mixtures (18 μL), containing all the materials except H3K4me2 peptide were first incubated for 5 minutes. Then, the reactions were initiated by adding 2 μl of 0.2 mM peptide solution to the assay mixtures. Absorbance at 515 nm was monitored for 30 minutes in a 384-well plate (Nunc) by using a microplate reader (SpectraMax M2^e; Molecular Devices). Enzyme activity was determined from the linear part of the reaction curve. The ratio of the enzyme activity measured in the presence of inhibitor to the activity of the control was plotted against log[Inh].

LSD2 Inhibition Assay. Production and purification of recombinant His-tagged human full-length LSD2 was performed as described previously.[21] The histone demethylation reaction for assaying LSD2 carried out for 1 hour at 37 C in 20 μL of 50 mM HEPES-NaOH (pH 8.5) containing 0.1% BSA, 2 μg of His-tagged full-length LSD2, and 10 μM H3K4me2, the chemically synthesized peptide consisted of the first 21 amino acid residues of histone H3, incorporating dimethylated lysine at position 4. The reaction was stopped by adding 20 μL of 100% acetonitrile including 0.1% trifluoroacetic acid. 0.5 μL of 10mg/ml α-Cyano-4-hydroxycinnamic acid was added to the 0.5 μL of reaction mixture, and 1 μL of this mixture was spotted on the sample plate, dried and analyzed by matrix-assisted laser desorption ionization time-of-flight mass spectrometry (MALDI-TOFMS) using JMS-S3000 (JEOL). The enzymatic removal of H3K4me0/1 from H3K4me2 substrate was quantified by this protocol. The LSD2 inhibition activity of the test compounds was calculated from the remaining amount of H3K4me2. The 50% inhibitory concentration (IC_{50}) of the test compounds was calculated as the concentration at which the half amount of H3K4me2 was removed compared to that removed when the enzyme was added.

MAO Inhibition Assays. The MAO activity assays were performed using a MAO-Glo™ assay kit (Promega), according to the supplier's protocol. MAO A (18 unit/mg) or MAO B (6 unit/mg) (Sigma-Aldrich) (25 μL/well), 160 μM (for MAO-A) or 16 μM (for MAO-B) (4*S*)-4,5-dihydro-2-(6-hydroxybenzothiazolyl)-4-thiazolecarboxylic acid (12.5 μL/well), a MAO substrate, and various concentrations of inhibitors (12.5 μL/well) were incubated at room temperature. Reactions were stopped after 60 min by adding reconstituted Luciferin Detection Reagent (50 μL/well). Then, 20 min after addition of this reagent, the fluorescence at 562 nm of the wells was measured with a fluorescence reader. The value of % inhibition was calculated from the fluorescence readings of inhibited wells relative to those of control wells.

JARID1A Inhibition Assay. The JARID1A activity was measured as described in ref 22.

Kinetic Analysis. The kinetic analysis was performed using a LSD1 fluorometric drug discovery kit (Enzo #NML-AK544-0001). Peptide **3**, H3K4me2 peptide (final concentration, 20 μM) and HRP/CELLestial Red were mixed in assay buffer (total volume, 80 μL) on each well of a 96-plate. The reactions (in 100 μL) were initiated by adding LSD1 (10 μg) in 20 μL of assay buffer to each well. After incubation at room temperature for 5 minutes, the fluorescence in each well was measured with an ARVO™ X3 microplate reader (excitation at 540 nm, emission, at 590 nm) every 30 seconds for 15 minutes.

MALDI-TOF/MS Analysis. LSD1 (12 μM) was incubated with 100 μM peptides **3** and **4** for 22 hours at room temperature in 50 mM sodium phosphate buffer (pH 7.5), 4% glycerol and 1% DMSO. The control was run with FAD instead of the enzyme. The reaction mixtures (10 μL) were then denatured with 6 M guanidine hydrochloride (10 μL) and acidified with 1% TFA (5 μL). An aliquot of the reaction mixture (10 μL) was desalted and concentrated using ZipTip μ-C18 (Millipore) (eluted with 5 μL of 50% MeCN containing 0.1% TFA). The eluate was

analyzed on a 5800 MALDI-TOF/TOF mass spectrometer (AB SCIEX). MALDI mass spectra were acquired between m/z 800 and 4000 in the positive ion mode. α-Cyano-4-hydroxycinnamic acid (CHCA, LaserBio) was used as the MALDI matrix without further purification. CHCA was dissolved in 50% MeCN containing 0.1% TFA to a concentration of 5 mg/mL. Samples for MALDI-TOF MS analysis were prepared by mixing the desalted reaction mixture (2 μL) with the matrix solution (2 μL). The applied samples (1 μL) were allowed to dry at room temperature.

Western Blot Analysis. Human cervical carcinoma HeLa cells were cultured in RPMI 1640 containing 10% heat-inactivated fetal bovine serum (FBS), penicillin and streptomycin mixture at 37 °C in a humidified atmosphere of 5% CO_2 in air. The HeLa cells (5×10^5) were plated in 6-well plates (Iwaki) and cultured for 24 hours. After removal of the medium, the cells were washed with PBS. The cells were incubated with synthetic peptides at the indicated concentrations in RPMI1640 medium without FBS for 24 hours, then collected and extracted with SDS buffer. Protein concentrations of the lysates were determined using a BCA protein assay. Equivalent amounts of protein from each lysate were resolved in 5–20% SDS-polyacrylamide gels and transferred onto PVDF membranes. After blocking with TBS-T containing 5% skim milk, the transblotted membranes were probed with rabbit monoclonal H3K4me3 antibody (Abcam, #ab8580) (1:500 dilution), rabbit polyclonal H3K4me2 antibody (Abcam, #ab32356) (1:1000 dilution), rabbit polyclonal H3K4me1 antibody (Abcam, #ab194691) (1:500 dilution), rabbit polyclonal H3K9me2 antibody (Abcam, #ab194680) (1:500 dilution) or rabbit polyclonal H3 antibody (Abcam, #ab1791) (1:200000 dilution) in TBS-T. Each probed membrane was washed with TBS-T, incubated with ECL rabbit IgG, HRP-linked whole antibody (GE Healthcare Life Sciences, #NA934) (1:2500 dilution), and again washed

with TBS-T. The immunoblots were visualized by enhanced chemiluminescence with Immobilon™ Western Chemiluminescent HRP Substrate (Millipore, #P90718).

Cell viability assay. The cells were plated in 96-well plates at the initial density of 1 x 10^3 cells/well (50 μL/well, HeLa) and incubated at 37°C. After 24 hours, the medium was removed and the cells were washed with PBS. The cells were incubated with synthetic peptides at the indicated concentrations in 50 μL of RPMI1640 medium without FBS for 24 hours. Then, 50 μL of RPMI1640 culture medium was added to each well and the plates were incubated at 37 °C under 5% CO_2 in air for a further 48 hours. The mixtures were then treated with 10 μL of AlamarBlue® (AbD Serotec, #BUF012A), and incubation was continued at 37 °C for 3 hours. The fluorescence in each well was measured with an ARVO™ X3 microplate reader (excitation at 540 nm, emission, at 590 nm). The cell viability (%) was calculated from the fluorescence readings.

ASSOCIATED CONTENT

Supporting Information

The Supporting Information is available free of charge on the ACS Publications website at DOI: 10.1021/acs.jmed-chem.XXXXXXX.

Figures S1–S24, Chiral HPLC data of the methyl ester compound derivatized from unnatural amino acid **29**, HPLC data, and MS spectra of synthetic peptides (PDF)

Molecular formula strings (CSV)

AUTHOR INFORMATION

Corresponding Authors

T.S.: suzukit@koto.kpu-m.ac.jp.

A.O.: aotaka@tokushima-u.ac.jp.

ACKNOWLEDGMENT

We thank Ms. Mie Tsuchida and Ms. Miho Hosoi for their technical support. This work was supported in part by JST CREST program (T.S.), a Grant-in-Aid for Scientific Research from the Japan Society for the Promotion of Science (T.S.), Takeda Science Foundation (T.S.), Mochida Memorial Foundation for Medical and Pharmaceutical Research (T.S.), Terumo Foundation for Life Science and Arts (Y.I.) and Kyoto-Funding for Innovation in Health-related R&D Fields (Y.I.)

ABBREVIATIONS

KDM, lysine demethylase; LSD, lysine-specific demethylase; FAD, flavin adenine dinucleotide; PCPA, phenylcyclopropylamine; JARID, Jumonji AT-rich interactive domain.

REFERENCES

(1) Kouzarides, T. Chromatin modifications and their function. *Cell* **2007**, *128*, 693–705.

(2) (a) Liu, L. J.; Lu, L.; Zhong, H. J.; He, B.; Kwong, D. W.; Ma, D. L.; Leung, C. H. An Iridium(III) Complex Inhibits JMJD2 Activities and Acts as a Potential Epigenetic Modulator. *J. Med. Chem.* **2015**, *58*, 6697–6703. (b) Zhong, H. J.; Lu, L.; Leung,K. H.; Wong, C. C. L.; Peng, C.; Yan, S. C.; Ma, D. L.; Cai, Z.; Wang, H. M. D.; Leung, C. H. An iridium(III)-based irreversible protein–protein interaction inhibitor of BRD4 as a potent anticancer agent. *Chem. Sci.* **2015**, *6*, 5400–5408. (c) Schnekenburger, M.; Dicato, M.; Diederich, M. Epigenetic modulators from "The Big Blue": a treasure to fight against cancer. *Cancer Lett.* **2014**, *351*, 182–197. (d) Lötsch, J.; Schneider, G.; Reker, D.; Parnham, M. J.; Schneider, P.; Geisslinger, G.; Doehring, A. Common non-epigenetic drugs as epigenetic modulators. *Trends Mol. Med.* **2013**, *19*, 742–753. (e) Knapp, S.; Weinmann, H. Small-molecule modulators for epigenetics targets. *ChemMedChem* **2013**, *8*, 1885–1891.

(3) Kubicek, S.; Jenuwein, T. A crack in histone lysine methylation. *Cell* **2004**, *119*, 903–906.

(4) (a) Shi, Y.; Lan, F.; Matson, C.; Mulligan, P.; Whetstine, J. R.; Cole, P.A.; Casero, R.A.; Shi, Y. Histone demethylation mediated by the nuclear amine oxidase homolog LSD1. *Cell* **2004**, *119*, 941–953. (b) Klose, R. J.; Kallin, E. M.; Zhang, Y. JmjC-domain-containing proteins and histone demethylation. *Nat. Rev. Genet.* **2006**, *7*, 715–727. (c) Shi, Y. Histone lysine demethylases: emerging roles in development, physiology and disease. *Nat. Rev. Genet.* **2007**, *8*, 829–833.

(5) Lee, M. G.; Wynder, C.; Cooch, N.; Shiekhattar, R. An essential role for CoREST in nucleosomal histone 3 lysine 4 demethylation. *Nature* **2005**, *437*, 432–435.

(6) (a) Schulte, J. H.; Lim, S.; Schramm, A.; Friedrichs, N.; Koster, J.; Versteeg, R.; Ora, I.; Pajtler, K.; Klein-Hitpass, L.; Kuhfittig-Kulle, S.; Metzger, E.; Schüle, R.; Eggert,

A.; Buettner, R.; Kirfel, J. Lysine-specific demethylase 1 is strongly expressed in poorly differentiated neuroblastoma: implications for therapy. *Cancer Res.* **2009**, *69*, 2065–2071. (b) Schenk, T.; Chen, W. C.; Göllner, S.; Howell, L.; Jin, L.; Hebestreit, K.; Klein, H. U.; Popescu, A. C.; Burnett, A.; Mills, K.; Casero, R. A. Jr.; Marton, L.; Woster, P.; Minden, M. D.; Dugas, M.; Wang, J. C.; Dick, J. E.; Müller-Tidow, C.; Petrie, K.; Zelent, A. Inhibition of the LSD1 (KDM1A) demethylase reactivates the all-trans-retinoic acid differentiation pathway in acute myeloid leukemia. *Nat. Med.* **2012**, *18*, 605–611.

(7) (a) Liang, Y.; Vogel, J. L.; Narayanan, A.; Peng, H.; Kristie, T. M. Inhibition of the histone demethylase LSD1 blocks α-herpesvirus lytic replication and reactivation from latency. *Nat. Med.* **2009**, *15*, 1312–1317.; (b) Shi, L.; Cui, S.; Engel, J. D.; Tanabe, O. Lysine-specific demethylase 1 is a therapeutic target for fetal hemoglobin induction. *Nat. Med.* **2013**, *19*, 291–294.

(8) Suzuki, T.; Miyata, N. Lysine demethylases inhibitors. *J. Med. Chem.* **2011**, *54*, 8236–8250.

(9) (a) Lin, Y.; Wu, Y.; Li, J.; Dong, C.; Ye, X.; Chi, Y. I.; Evers, B. M.; Zhou, B. P. The SNAG domain of Snail1 functions as a molecular hook for recruiting lysine-specific demethylase 1. *EMBO J.* **2010**, *29*, 1803–1816. (b) Lin, T.; Ponn, A.; Hu, X.; Law, B. K.; Lu, J. Requirement of the histone demethylase LSD1 in Snai1-mediated transcriptional repression during epithelial-mesenchymal transition. *Oncogene* **2010**, *29*, 4896–4904.

(10) Ferrari-Amorotti, G.; Fragliasso, V.; Esteki, R.; Prudente, Z.; Soliera, A. R.; Cattelani, S.; Manzotti, G.; Grisendi, G.; Dominici, M.; Pieraccioli, M.; Raschellà, G.; Chiodoni, C.; Colombo, M. P.; Calabretta, B. Inhibiting interactions of lysine demethylase LSD1 with snail/slug blocks cancer cell invasion. *Cancer Res.* **2013**, *73*, 235–245.

(11) Tortorici, M.; Borrello, M. T.; Tardugno, M.; Chiarelli, L. R.; Pilotto, S.; Ciossani, G.; Vellore, N. A.; Bailey, S. G.; Cowan, J.; O'Connell, M.; Crabb, S. J.; Packham, G.; Mai,

A.; Baron, R.; Ganesan, A.; Mattevi, A. Protein recognition by short peptide reversible inhibitors of the chromatin-modifying LSD1/CoREST lysine demethylase. *ACS Chem. Biol.* **2013**, *8*, 1677–1682.

(12) (a) Itoh, Y.; Suzuki, T.; Miyata, N. Small-molecular modulators of cancer-associated epigenetic mechanisms. *Mol. Biosyst.* **2013**, *9*, 873–896. (b) Schmidt, D. M.; McCafferty, D. G. *trans*-2-Phenylcyclopropylamine is a mechanism-based inactivator of the histone demethylase LSD1. *Biochemistry* **2007**, *46*, 4408–4416. (c) Yang, M.; Culhane, J. C.; Szewczuk, L. M.; Jalili, P.; Ball, H. L.; Machius, M.; Cole, P. A.; Yu, H. Structural basis for the inhibition of the LSD1 histone demethylase by the antidepressant *trans*-2-phenylcyclopropylamine. *Biochemistry* **2007**, *46*, 8058–8065. (d) Ueda, R.; Suzuki, T.; Mino, K.; Tsumoto, H.; Nakagawa, H.; Hasegawa, M.; Sasaki, R.; Mizukami, T.; Miyata, N. Identification of cell-active lysine specific demethylase 1-selective inhibitors. *J. Am. Chem. Soc.* **2009**, *131*, 17536–17537. (e) Ogasawara, D.; Suzuki, T.; Mino, K.; Ueda, R.; Khan, M. N.; Matsubara, T.; Koseki, K.; Hasegawa, M.; Sasaki, R.; Nakagawa, H.; Mizukami, T.; Miyata, N. Synthesis and biological activity of optically active NCL-1, a lysine-specific demethylase 1 selective inhibitor. *Bioorg. Med. Chem.* **2010**, *19*, 3702–3708. (f) Ogasawara, D.; Itoh, Y.; Tsumoto, H.; Kakizawa, T.; Mino, K.; Fukuhara, K.; Nakagawa, H.; Hasegawa, M.; Sasaki, R.; Mizukami, T.; Miyata, N.; Suzuki, T. Lysine-specific demethylase 1-selective inactivators: protein-targeted drug delivery mechanism. *Angew. Chem. Int. Ed.* **2013**, *52*, 8620–8624. (g) Binda, C.; Valente, S.; Romanenghi, M.; Pilotto, S.; Cirilli, R.; Karytinos, A.; Ciossani, G.; Botrugno, O. A.; Forneris, F.; Tardugno, M.; Edmondson, D. E.; Minucci, S.; Mattevi, A.; Mai, A. Biochemical, structural, and biological evaluation of tranylcypromine derivatives as inhibitors of histone demethylases LSD1 and LSD2. *J. Am. Chem. Soc.* **2010**, *132*, 6827–6833. (h) Mimasu, S.; Umezawa, N.; Sato, S.; Higuchi, T.;

Umehara, T.; Yokoyama, S. Structurally designed *trans*-2-phenylcyclopropylamine derivatives potently inhibit histone demethylase LSD1/KDM1. *Biochemistry* **2010**, *49*, 6494–6503. (i) Culhane, J. C.; Wang, D.; Yen, P. M.; Cole, P. A. Comparative analysis of small molecules and histone substrate analogues as LSD1 lysine demethylase inhibitors. *J. Am. Chem. Soc.* **2010**, *132*, 3164–3176. (j) Metzger, E.; Wissmann, M.; Yin, N.; Müller, J. M.; Schneider, R.; Peters, A. H.; Günther, T.; Buettner, R.; Schüle, R. LSD1 demethylates repressive histone marks to promote androgen-receptor-dependent transcription. *Nature* **2005**, *437*, 436–439. (k) Schmitt, M. L.; Hauser, A. T.; Carlino, L.; Pippel, M.; Schulz-Fincke, J.; Metzger, E.; Willmann, D.; Yiu, T.; Barton, M.; Schüle, R.; Sippl, W.; Jung, M. Nonpeptidic propargylamines as inhibitors of lysine specific demethylase 1 (LSD1) with cellular activity. *J. Med. Chem.* **2013**, *56*, 7334–7342. (l) Prusevich, P.; Kalin, J. H.; Ming, S. A.; Basso, M.; Givens, J.; Li, X.; Hu, J.; Taylor, M. S.; Cieniewicz, A. M.; Hsiao, P. Y.; Huang, R.; Roberson, H.; Adejola, N.; Avery, L. B.; Casero, R. A. Jr.; Taverna, S. D.; Qian, J.; Tackett, A. J.; Ratan, R. R.; McDonald, O. G.; Feinberg, A. P.; Cole, P. A. A selective phenelzine analogue inhibitor of histone demethylase LSD1. *ACS Chem. Biol.* **2014**, *9*, 1284–1293. (m) Kakizawa, T.; Ota, Y.; Itoh, Y.; Tsumoto, H.; Suzuki T. Histone H3 peptide based LSD1-selective inhibitors. *Bioorg. Med. Chem. Lett.* **2015**, *25*, 1925–1928. (n) Khan, MNA.; Tsumoto, H.; Itoh, Y.; Ota, Y.; Suzuki, M.; Ogasawara, D.; Nakagawa, H.; Mizukami, T.; Miyata, N.; Suzuki, T. Design, synthesis, and biological activity of N-alkylated analogue of NCL1, a selective inhibitor of lysine-specific demethylase 1. *MedChemComm* **2015**, *6*, 407–412. (o) Itoh, Y.; Ogasawara, D.; Ota, Y.; Mizukami, T.; Suzuki, T. Synthesis, LSD1 inhibitory activity, and LSD1 binding model of optically pure lysine-PCPA conjugates. *Comput. Struct. Biotechnol. J.* **2014**, *9*, e201402002. (p) Mohammad, H. P.; Smitheman, K. N.; Kamat, C. D.; Soong, D.; Federowicz, K. E.; Van

Aller, G. S.; Schneck, J. L.; Carson, J. D.; Liu, Y.; Butticello, M.; Bonnette, W. G.; Gorman, S. A.; Degenhardt, Y.; Bai, Y.; McCabe, M. T.; Pappalardi, M. B.; Kasparec, J.; Tian, X.; McNulty, K. C.; Rouse, M.; McDevitt, P.; Ho, T.; Crouthamel, M.; Hart, T. K.; Concha, N. O.; McHugh, C. F.; Miller, W. H.; Dhanak, D.; Tummino, P. J.; Carpenter, C. L.; Johnson, N. W.; Hann, C. L.; Kruger, R. G. A DNA Hypomethylation Signature Predicts Antitumor Activity of LSD1 Inhibitors in SCLC. *Cancer Cell* **2015**, *28*, 57–69.

(13) Copeland, R. A.; Pompliano, D. L.; Meek, T. D. Drug-target residence time and its implications for lead optimization. *Nat. Rev. Drug Discov.* **2006**, *5*, 730−739.

(14) Ito, Y.; Yoshimatsu, M. Metal-free reductive cyclization and isomerization of sulfanyl-1,6-diynes using sodium borohydride. *Chem. Lett.* **2014**, *43*, 1758–1760.

(15) (a) Lee, M. M.; Fekner, T.; Tang, T. H.; Wang, L.; Chan, A. H.; Hsu, P. H.; Au, S. W.; Chan, M. K. A click-and-release pyrrolysine analogue. *ChemBioChem* **2013**, *14*, 805−808. (b) Shetty, D.; Jeong, J. M.; Ju, C. H.; Kim, Y.; Lee, J. Y.; Lee, Y. S.; Lee, D. S.; Chung, J. K.; Lee, M. C. Synthesis and evaluation of macrocyclic amino acid derivatives for tumor imaging by gallium-68 positron emission tomography. *Bioorg. Med. Chem.* **2010**, *18*, 7338−7347.

(16) Baron, R.; Binda, C.; Tortorici, M.; McCammon, J. A.; Mattevi, A. Molecular mimicry and ligand recognition in binding and catalysis by the histone demethylase LSD1-CoREST complex. *Structure* **2011**, *19*, 212–220.

(17) (a) Culhane, J. C.; Szewczuk, L. M.; Liu, X.; Da, G.; Marmorstein, R.; Cole, P. A. A mechanism-based inactivator for histone demethylase LSD1. *J. Am. Chem. Soc.* **2006**, *128*, 4536–4537. (b) Yang, M.; Culhane, J. C.; Szewczuk, L. M.; Gocke, C. B.; Brautigam, C. A.; Tomchick, D. R.; Machius, M.; Cole, P. A.; Yu, H. Structural basis of histone demethylation by LSD1 revealed by suicide inactivation. *Nat. Struct. Mol. Biol.* **2007**, *14*, 535–539.

(18) Christensen, J.; Agger, K.; Cloos, P. A.; Pasini, D.; Rose, S.; Sennels, L.; Rappsilber, J.; Hansen, K. H.; Salcini, A. E.; Helin, K. RBP2 belongs to a family of demethylases, specific for tri-and dimethylated lysine 4 on histone 3. *Cell* **2007**, *128*, 1063–1076.

(19) Futaki, S.; Suzuki, T.; Ohashi, W.; Yagami, T.; Tanaka, S.; Ueda, K.; Sugiura, Y. Arginine-rich peptides. An abundant source of membrane-permeable peptides having potential as carriers for intracellular protein delivery. *J. Biol. Chem.* **2001**, *276*, 5836–5840.

(20) Hashimoto, N.; Aoyama T., Shioiri, T. New methods and reagents in organic synthesis. 14. A simple efficient preparation of methyl esters with trimethylsilyldiazomethane ($TMSCHN_2$) and itsaApplication to gas chromatographic analysis of fatty acids. *Chem. Pharm. Bull.* **1981**, *29*, 1475–1478.

(21) Mino, K.; Nishimura, S.; Ninomiya, S.; Tujii, H.; Matsumori, Y.; Tsuchida, M.; Hosoi, M.; Koseki, K.; Wada, S.; Hasegawa, M.; Sasaki, R.; Murakami-Yamaguchi, Y.; Narita, H.; Suzuki, T.; Miyata, N.; Mizukami, T. Regulation of tissue factor pathway inhibitor-2 (TFPI-2) expression by lysine-specific demethylase 1 and 2 (LSD1 and LSD2). *Biosci. Biotechnol. Biochem.* **2014**, *78*, 1010–1017.

(22) (a) Suzuki, T.; Ozasa, H.; Itoh, Y.; Zhan, P.; Sawada, H.; Mino, K.; Walport, L.; Ohkubo, R.; Kawamura, A.; Yonezawa, M.; Tsukada, Y.; Tumber, A.; Nakagawa, H.; Hasegawa, M.; Sasaki, R.; Mizukami, T.; Schofield, C. J.; Miyata N. Identification of the KDM2/7 histone lysine demethylase subfamily inhibitor and its antiproliferative activity. *J. Med. Chem.* **2013**, *56*, 7222−7231. (b) Itoh, Y.; Sawada, H.; Suzuki, M.; Tojo, T.; Sasaki, R.; Hasegawa, M.; Mizukami, T.; Suzuki, T. Identification of jumonji AT-rich interactive domain 1A inhibitors and their effect on cancer cells. *ACS Med. Chem. Lett.* **2015**, *6*, 665−670.

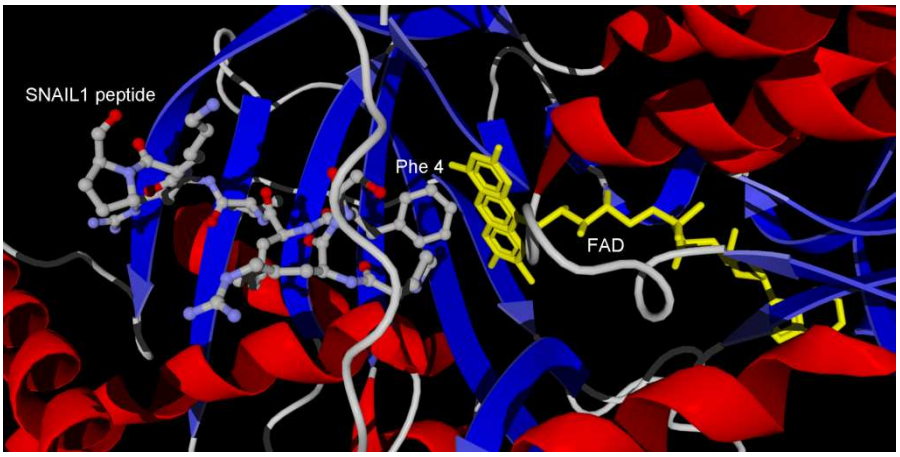

Figure 1. X-ray crystal structure of LSD1 complex with a SNAIL1 peptide (PDB code 2Y48). FAD and the SNAIL1 peptide are displayed as tube and ball-and-stick models, respectively.

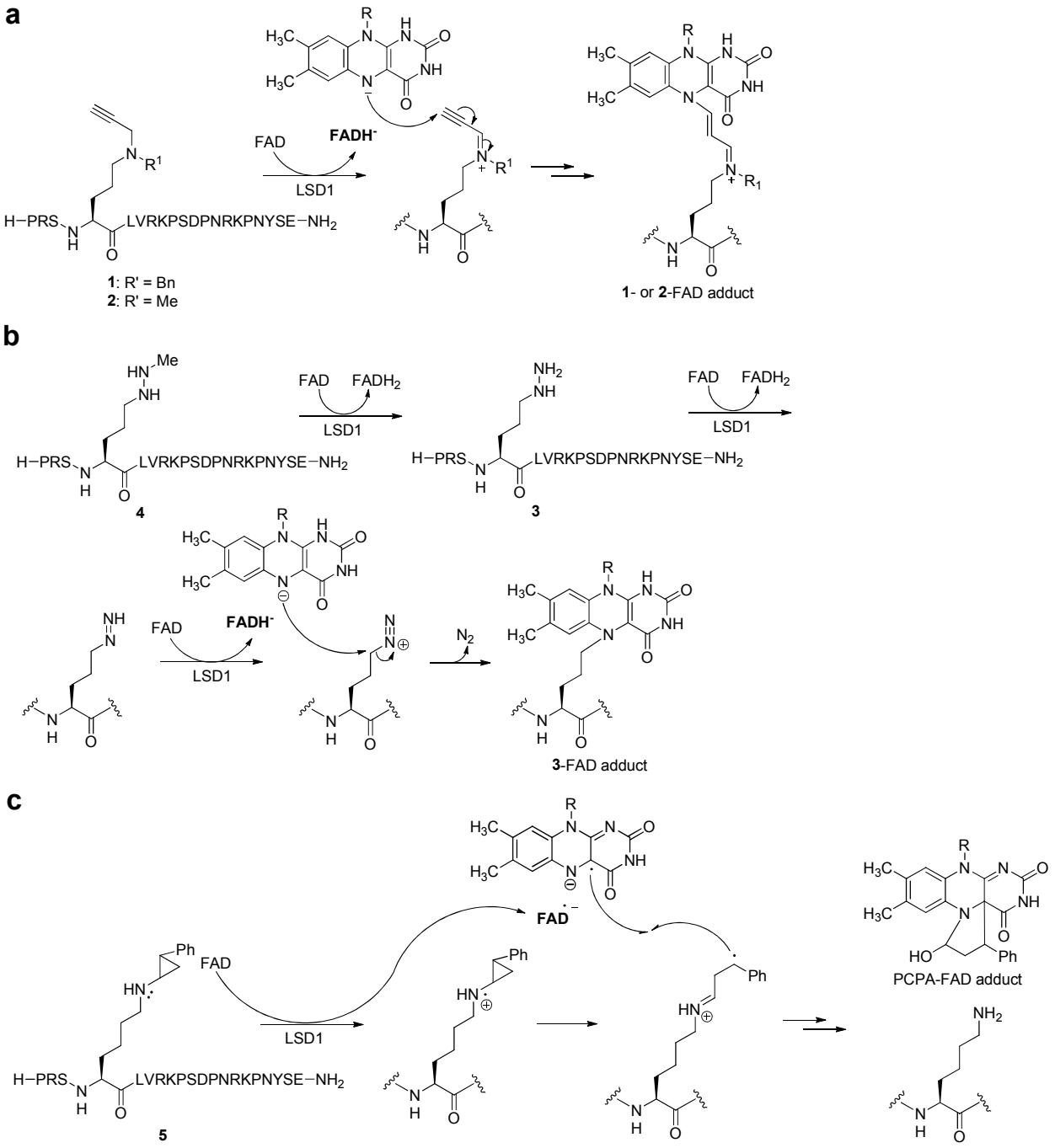

Figure 2. (a) Plausible mechanism of inactivation of LSD1 by *N*-propargyl lysine peptide **1** or **2**. (b) Plausible mechanism of inactivation of LSD1 by peptides **3** and and **4** bearing a hydrazine moiety. (c) Plausible mechanism of inactivation of LSD1 by peptide **5** bearing a PCPA moiety.

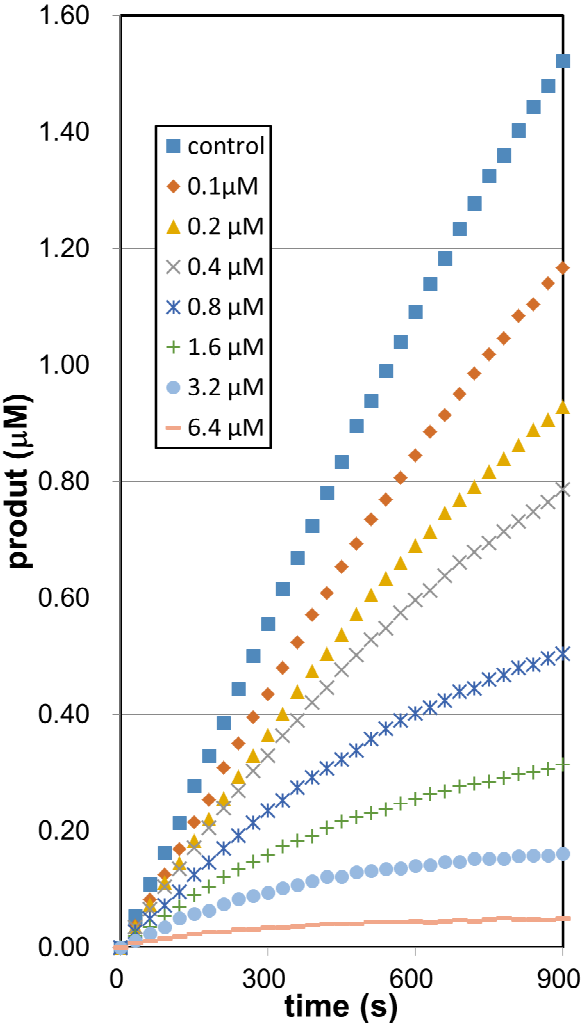

Figure 3. Time- and concentration-dependent inhibition of LSD1 by peptide **3**. Steady-state progress curves obtained for inactivation of LSD1 by 0 (■), 0.1 (♦) 0.2 (▲), 0.4 (×), 0.8 (*), 1.6 (+), 3.2 (●), and 6.4 (-) μM **3**.

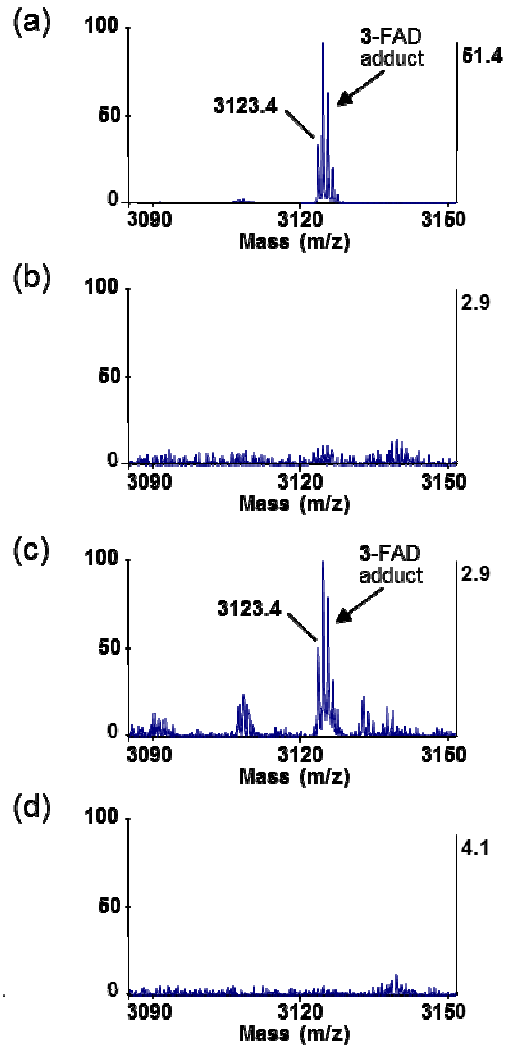

Figure 4. Mass spectrometric detection of **3**-FAD adduct. Mass spectra (positive mode) were obtained from (a) LSD1-**3** mixture, (b) FAD-**3** mixture in the absence of LSD1 and (c) LSD1-**4** mixture, and (d) FAD-**4** mixture in the absence of LSD1.

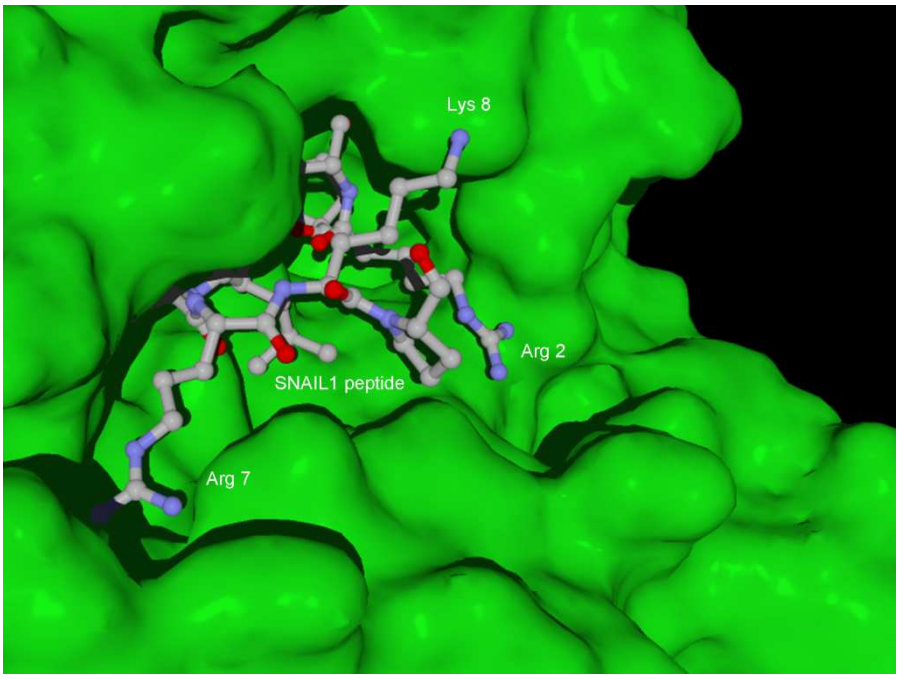

Figure 5. Surface of the catalytic pocket of LSD1 in complex with a SNAIL1 peptide (PDB code 2Y48). The SNAIL1 peptide is displayed as a ball-and-stick model.

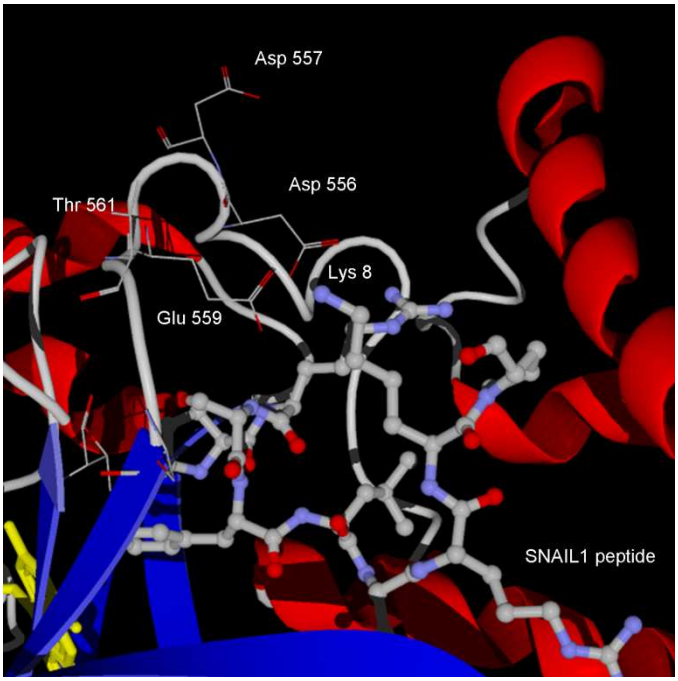

Figure 6. View of the catalytic pocket of LSD1 in the complex with a SNAIL1 peptide (PDB code 2Y48).

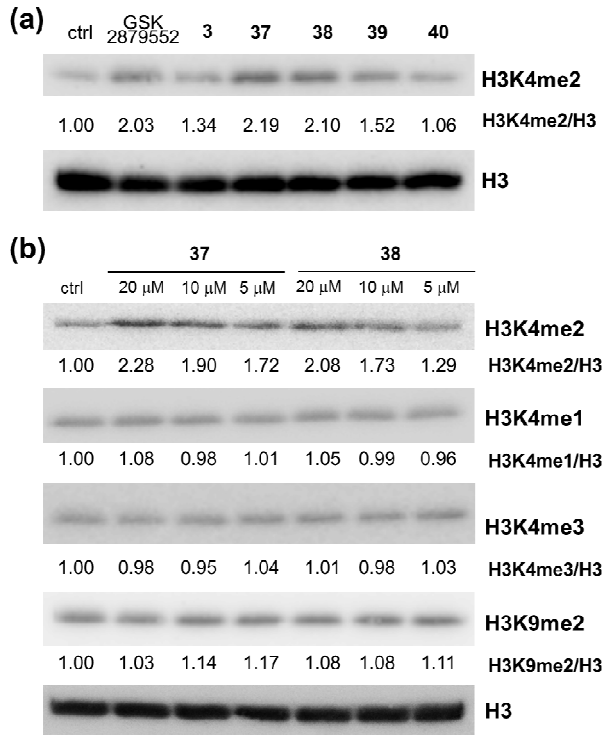

Figure 7. Western blot detection of methylation levels of H3K4 or H3K9 in HeLa cells after 24 h treatment with peptides in the absence of fetal bovine serum (FBS). Values of H3K4me2/H3, H3K4me1/H3, H3K4me3/H3, or H3K9me2/H3 ratio determined by optical density measurement of the blots are shown. (a) Treatment with 20 μM of GSK2879552, peptides **3**, and **37**–**40**. (b) Dose-dependency for peptides **37** and **38**.

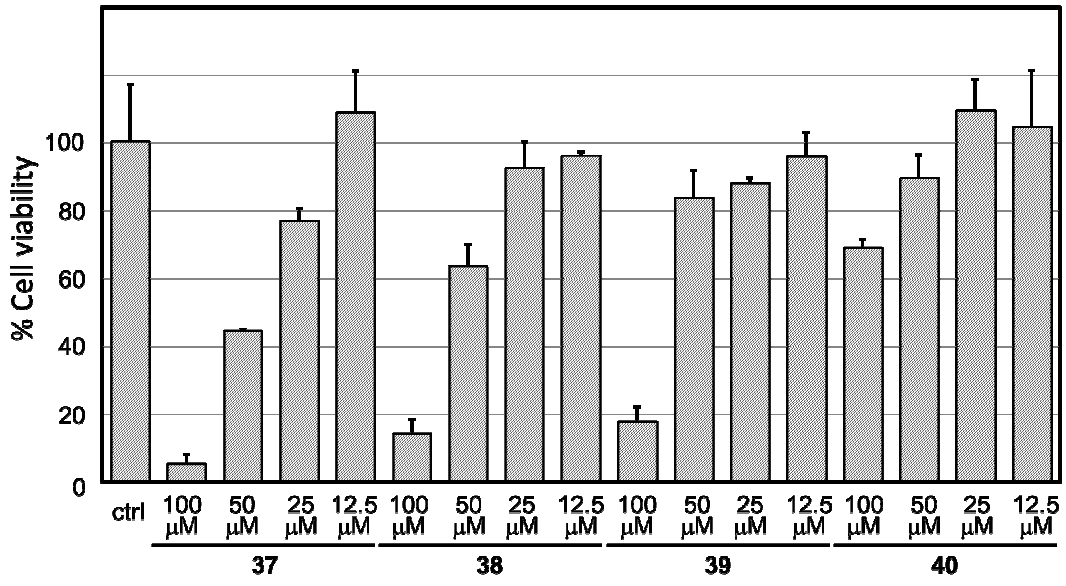

Figure 8. Effect of peptides **37**–**40** on viability of HeLa cells. The cells were incubated for 48 h after 24 h treatment with peptides **37**–**40** at the indicated concentrations in the absence of fetal bovine serum (FBS). Error bars represent the mean standard deviation (SD) of at least three samples. 300 μM GSK2879552 reduced the cell viability by 9.96 ± 0.47% (GSK2879552 was inactive at 100 μM).

Scheme 1. Synthesis of Peptides 1 and 2.[a]

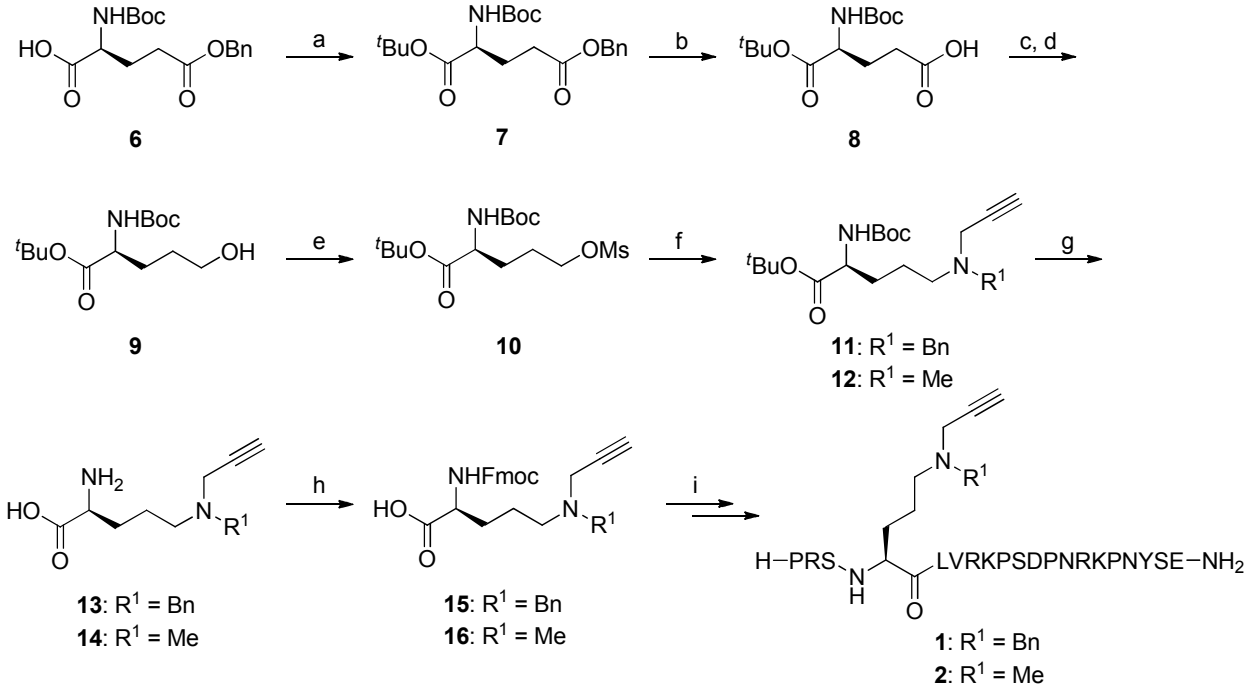

[a] Reagents and conditions: (a) ^{t}BuOH, EDCI, DMAP, CH_2Cl_2, room temp, 93%; (b) H_2, Pd/C, MeOH, room temp, 97%; (c) ClCOOEt, Et_3N, THF, –10 °C; (d) $NaBH_4$, THF, H_2O, 0 °C to room temp, 74% (two steps); (e) MsCl, Et_3N, DMAP, CH_2Cl_2, –20 °C, 58%; (f) *N*-benzylpropargylamine or *N*-methylpropargylamine, Cs_2CO_3 for **11** or Et_3N, DMAP for **12**, DMF, 65 °C for **11** or 75 °C for **12**, 19% for **11**, 23% for **12**; (g) HCl, 1,4-dioxane, CH_2Cl_2, 0 °C to room temp, 88% for **13**, 92% for **14**; (h) Fmoc-OSu, $NaHCO_3$, 1,4-dioxane, H_2O, 0 °C to room temp, 20% for **15**, 19% for **16**; (i) Fmoc-based solid-phase peptide synthesis, 17% for **1**, 16% for **2**.

Scheme 2. Synthesis of Peptides 3 and 4.[a]

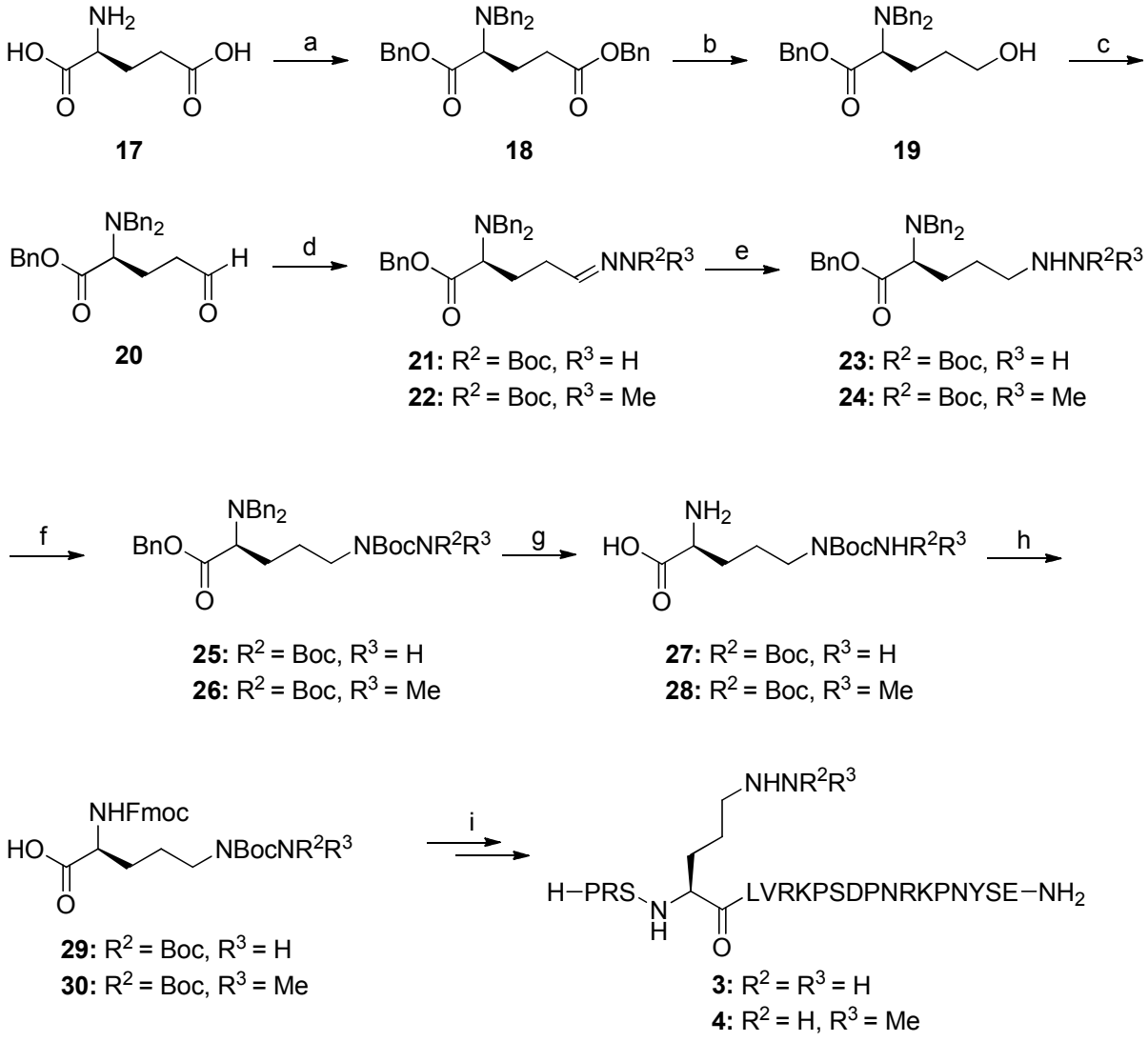

[a]Reagents and conditions: (a) BnBr, K_2CO_3, NaOH, H_2O, reflux, 29%; (b) DIBAL, THF, –10 to 0 °C, 92%; (c) DMSO, $(COCl)_2$, Et_3N, CH_2Cl_2, –78 °C, 85%; (d) $R^2R^3NNH_2$, THF, room temp, 94% for **21**, 93% for **22**; (e) $NaBH_3CN$, EtOH, AcOH, room temp, 69% for **23**, 92% for **24**; (f) $(Boc)_2O$, DMAP, CH_2Cl_2, room temp, 92% for **25**, 40% for **26**; (g) Pd black, HCOOH, MeOH, –40 °C to room temp; (h) Fmoc-OSu, $NaHCO_3$, 1,4-dioxane, H_2O, 0 °C to room temp, 89% for **29** (2 steps), 82% for **30** (2 steps); (i) Fmoc-based solid-phase peptide synthesis, 16% for **3**, 29% for **4**.

Scheme 3. Synthesis of Peptide 5.[a]

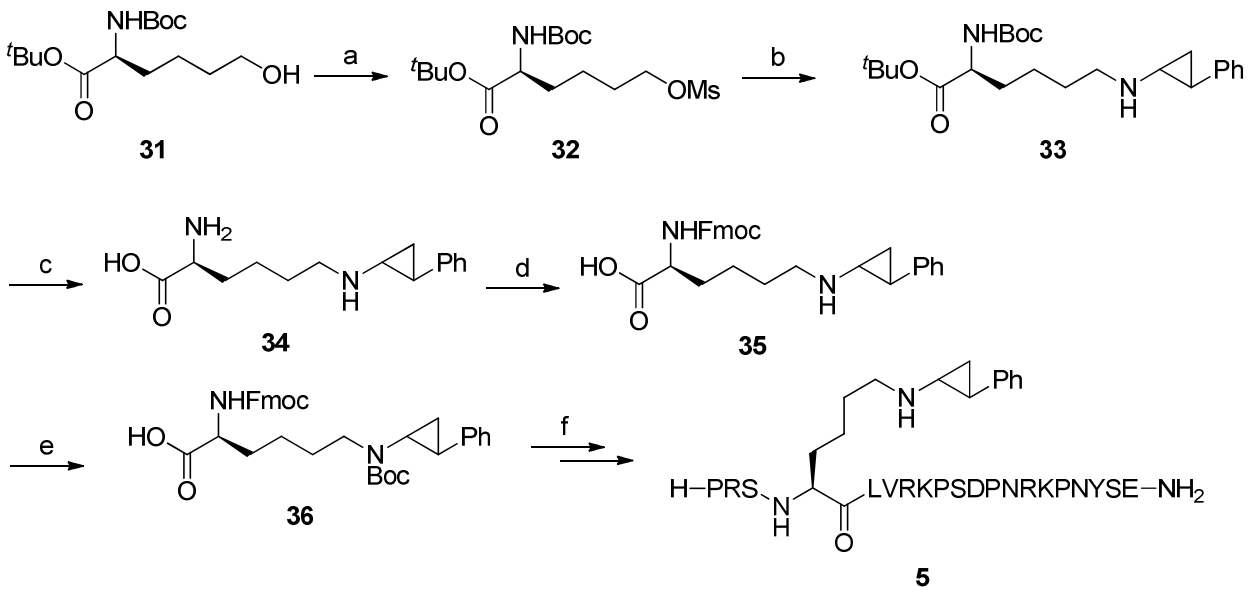

[a]Reagents and conditions: (a) MsCl, Et_3N, DMAP, CH_2Cl_2, –20 °C, 66%; (b) PCPA, Cs_2CO_3, DMF, 75°C, 75%; (c) HCl, dioxane, 0 °C to room temp, 78%; (d) FmocCl, $NaHCO_3$, 1,4-dioxane, H_2O, 0 °C to room temp, 14 %; (e) $(Boc)_2O$, $NaHCO_3$, 1,4-dioxane, H_2O, 0 °C to room temp, 28%; (g) Fmoc-based solid-phase peptide synthesis, 14%.

Chart 1. Examples of Reported Small-molecular LSD1 Inactivators.

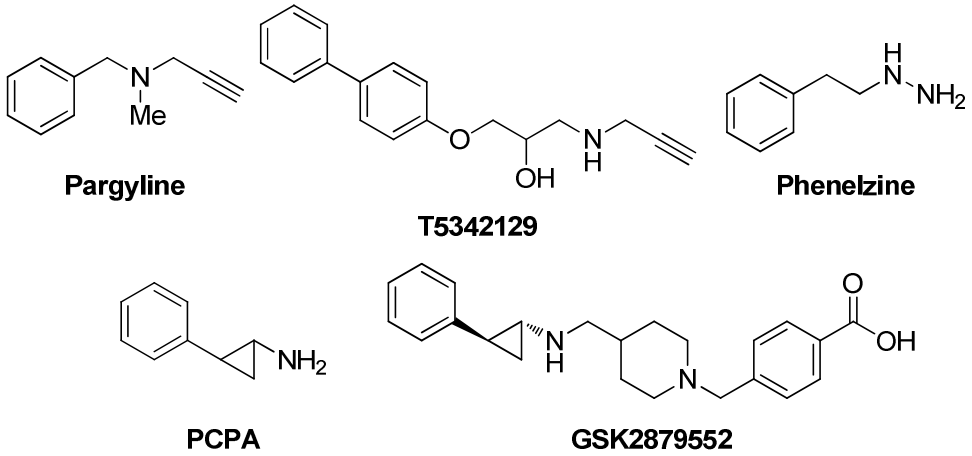

Chart 2. Structures of SNAIL1-Based Peptides 1–5.

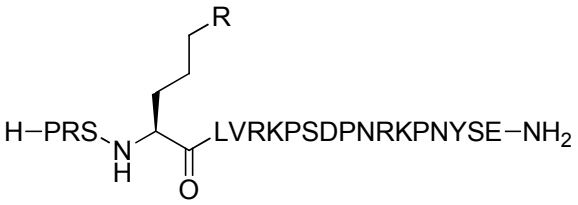

1: R = 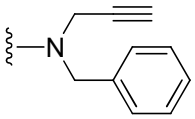

2: R = 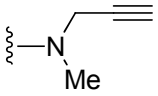

3: R = —$NHNH_2$

4: R = —NHNHMe

5: R = 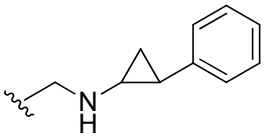

Chart 3. Structures of oligoarginine-conjugated peptides 37–40.

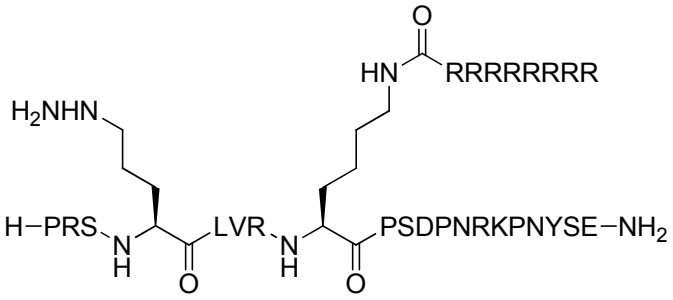

37

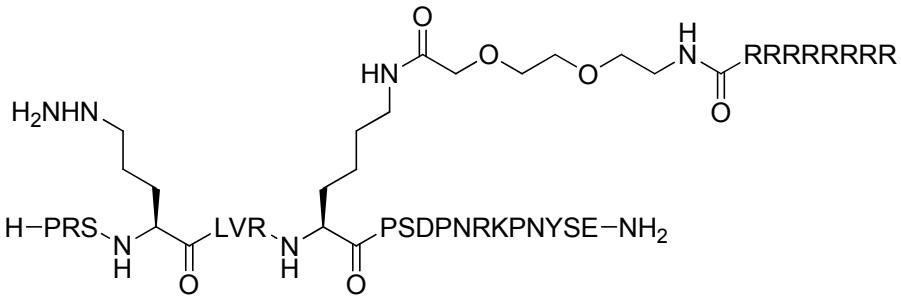

38

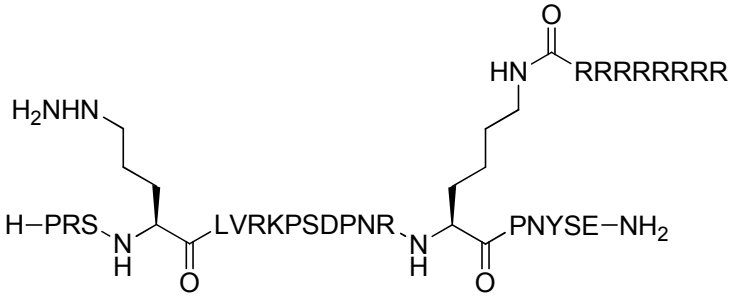

39

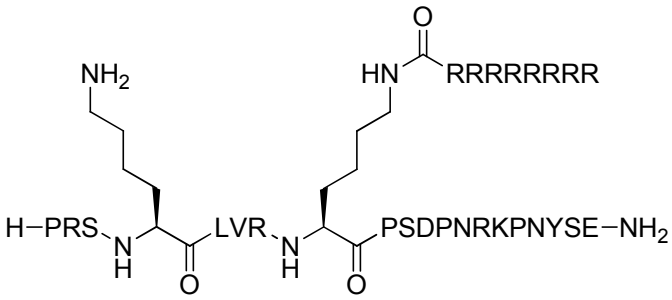

40

Table 1. In vitro LSD1-, LSD2-, MAO-A-, MAO-B-, and JARID1A-inhibitory activities of SNAIL1-based peptides 1–5.[a,b]

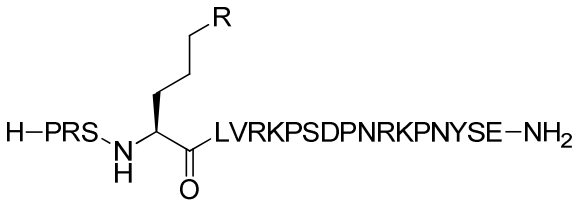

Compound	R	IC_{50} (μM)				
		LSD1	LSD2	MAO A	MAO B	JARID1A
1	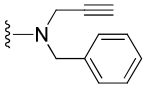	40	N.D.[c]	N.D.	N.D.	N.D.
2	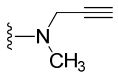	17	N.D.	N.D.	N.D.	N.D.
3	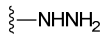	0.44	>50	>30	>30	>50
4		8.40	>50	>30	>30	>50
5	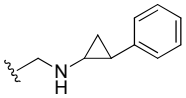	63	N.D.	N.D.	N.D.	N.D.

[a]Values are means of at least two experiments. [b]PCPA (IC_{50} = 41 μM for LSD1; IC_{50} = 4.2 μM for MAO A; IC_{50} = 3.5 μM for MAO B) and GSK2879552 (IC_{50} = 0.61 μM for LSD1) were used as positive controls. [c]N.D. = Not determined.

Table 2. In vitro LSD1-, LSD2-, MAO-A-, MAO-B-, and JARID1A-inhibitory activities of oligoarginine-conjugated peptides 37–39.[a,b]

Compound	IC_{50} (μM)				
	LSD1	LSD2	MAO A	MAO B	JARID1A
3	0.44	>50	>30	>30	>50
37	0.28	13.20	>30	29	6.74
38	0.29	23.20	>30	30	12.9
39	0.32	7.51	>30	30	5.05

[a]Values are means of at least three experiments. [b]PCPA (IC_{50} = 41 μM for LSD1; IC_{50} = 4.2 μM for MAO A; IC_{50} = 3.5 μM for MAO B) and GSK2879552 (IC_{50} = 0.61 μM for LSD1) were used as positive controls. [c]N.D. = Not determined.

TOC graphic

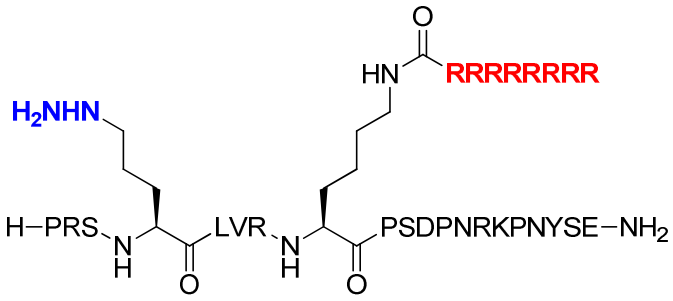

37

Cell-active SNAIL1 peptide-based LSD1 inactivator